

nucl-th/0404073
 TUM-T39-04-05
 23rd April 2004
 Submitted to Nuclear Physics **A**

Improved Convergence in the Three-Nucleon System at Very Low Energies

Harald W. Grießhammer^{a,b,1}

^a Institut für Theoretische Physik (T39), Physik-Department,
 Technische Universität München, D-85747 Garching, Germany

^b ECT*, Villa Tambosi, I-38050 Villazzano (Trento), Italy

Abstract

Neutron-deuteron scattering in the context of “pion-less” Effective Field Theory at very low energies is investigated to next-to-next-to-leading order. Convergence is improved by fitting the two-nucleon contact interactions to the tail of the deuteron wave-function, a procedure known as Z-parameterisation and extended here to the three-nucleon system. The improvement is particularly striking in the doublet-S wave (triton) channel, where better agreement to potential-model calculation and better convergence from order to order in the power counting is achieved for momenta as high as ~ 120 MeV. Investigating the cut-off dependence of the phase-shifts, one confirms numerically the analytical finding that the first momentum-dependent three-body force enters at N^2LO . The other partial waves converge also substantially faster. Effective-range parameters of the nd -system are determined, e.g. for the quartet-S-wave scattering length $a_q = [6.35 \pm 0.02]$ fm, which compares favourably both in magnitude and uncertainty with recent high-precision potential-model determinations. Differential cross-sections up to $E_{\text{lab}} \approx 15$ MeV agree with data.

Suggested PACS numbers: 11.80.Jy, 13.75.Cs, 14.20.Dh, 21.30.-x, 25.40.Dn, 27.10.+h

Suggested Keywords: Effective Field Theory, three-body system, three-body force, Faddeev equation, partial waves.

¹Email: hgrie@physik.tu-muenchen.de; permanent address: a

1 Introduction

The few-nucleon system at very low energies is an important tool to understand key physical questions. On the one hand, a new generation of high-precision experiments at the lower end of the energy spectrum use both polarised targets and beams, and employ neutrino detectors or radioactive-beam facilities to extract e.g. neutron properties, neutrino masses and reactions relevant for nuclear astro-physics. On the other hand, a plethora of pivotal physical processes is hard to access directly in experiments, like reaction rates in Big-Bang nucleo-synthesis. In both cases, it is mandatory that binding effects in light nuclei are taken into account with as few bias as possible towards a particular model of the few-nucleon system. Theory must provide such model-independent extraction and calibration methods or predictions at very low energies, often well below 20 MeV.

While *precision* – the numerical stability of computations – can be controlled by combining sophisticated algorithms with Moore’s law [1] and is hence (albeit sometimes formidable) not a fundamental problem, the necessary *accuracy* – namely an estimate of the systematic uncertainties of a theoretical ansatz – is harder to win and mandates understanding the physical system at hand. In the three-nucleon sector, this calls in particular for a systematic understanding of the rôle three-nucleon forces play. Traditionally, these were often introduced *a posteriori* to cure discrepancies between data and calculations, e.g. for the triton binding energy, but such a path is of course untenable when data are scarce or absent. There is also a host of deviations between experiment and theory for which a suitable three-body force could not yet be constructed, like the famed A_y -problem [2].

The so-called “pion-less” version of Effective Field Theory in Nuclear Physics (EFT(\not{p})) aspires to provide just such a systematic classification of all forces [3]. At its heart lies the tenet that Physics at those very low energies can be described by point-like interactions between nucleons only: One cannot identify pions as the lightest exchange-particles between nucleons as long as the typical external momentum p_{typ} in a reaction is below the pion mass m_π because the Compton wave-lengths are not small enough to resolve the nuclear forces as originating in part from one-pion exchange. With all particles but the nucleons thus “integrated out” as heavy, one can identify a small, dimension-less parameter $Q = \frac{p_{\text{typ}}}{\Lambda_{\not{p}}} \ll 1$, where $\Lambda_{\not{p}} \sim m_\pi$ is the typical momentum scale at which the one-pion exchange is resolved and EFT(\not{p}) must break down. The resultant power-counting orders each process according to the power in Q at which it starts to contribute and establishes therefore an ordering scheme which is used for systematically improvable, rigorous error estimates. This and the systematic, gauge invariant inclusion of external electro-weak currents and relativistic effects distinguishes EFT(\not{p}) from its historical roots, the Effective Range Expansion [4] and the model-independent approach to three-body physics [5].

EFT(\not{p}) is a mathematically well-defined, systematic low-energy theory of QCD. It is computationally considerably simpler than potential models or the “pion-ful” version of EFT, which attempts to extend Chiral Perturbation Theory to the few-nucleon system [6, 7, 8]. Conceptually, many problems which are also found when formulating a fully consistent “pion-ful” EFT are encountered in a simpler setting. It was used quite successfully to provide model-independent results for a cornucopia of two-nucleon processes with external

electro-weak probes, see the reviews [9, 10, 11] and references therein. Recently, a rigorous power-counting was developed for the three-nucleon forces in this approach, opening the path to new high-accuracy extractions and predictions of nucleonic and nuclear properties [12]. Now, convergence issues become interesting. They are the subject of this article.

In EFT(\not{p}), the strengthes of the contact interactions between the nucleons can be determined from low-energy observables in various ways, which differ in principle only by higher-order effects. Still, it is standard practise to to improve the speed of convergence by physical considerations. One would for example not try to describe deuteron properties by starting from the Effective Range Expansion (ERE) in the 3S_1 -channel of NN -scattering around zero momentum, in which the correct position of the deuteron pole at $B_t = 2.2246\dots$ MeV is reached only perturbatively. Instead, it is prudent to put the deuteron pole-position in the right place, and give the pole its correct strength. The deuteron wave-function has then the proper asymptotic fall-off and normalisation. Phillips et al. [13] showed that this *Z-parameterisation*¹ is an effective way to sum up the dominant effective-range contributions. It both simplifies calculations of deuteron properties and improves convergence.

As the 3S_1 -channel of NN -scattering is an important sub-cluster of the three-nucleon system, it is natural to consider the implications of this choice for the triton and other partial waves. With a slight extension, it can be included into the standard EFT treatment of the three-nucleon system in which an auxiliary two-nucleon field is introduced to simplify computations. This article will show that not only is the convergence both from order to order in the expansion and to experimental phase-shifts greatly improved; its results support also the power counting for the three-body forces pertinent to the triton – mathematically rigorously proven in [12] – by an error analysis of the $^2S_{\frac{1}{2}}$ -channel.

This article is organised as follows: The next Section merges Z-parameterisation with the auxiliary-field method. After a brief review of the formalism to compute Nd scattering in EFT(\not{p}) and the occurrence of three-body forces in the triton channel at the beginning of Section 3, the results for the $^2S_{\frac{1}{2}}$ -channel, triton properties and the Phillips line are examined in Sub-Sect. 3.3. I touch upon the pros and cons of including the effective range as leading-order in Sect. 3.4. Finally, the effect of Z-parameterisation on the other partial waves of the Nd -system is discussed in Sub-Sect. 3.5. Various effective-range parameters of low partial waves are also listed, together with comparisons between experimental and theoretical cross-sections. The Conclusions in Sect. 4 are followed by an Appendix on the derivation of the three-body equations in EFT(\not{p}), defining also the spin-isospin projection operators in the three-nucleon system.

¹Pronounced “Zed-parameterisation”.

2 Z-Parameterisation and Auxiliary-Field-Formalism in the Two-Nucleon System

2.1 Merging the Auxiliary Field Formalism . . .

It is a standard technique to simplify calculations in EFT(\not{p}) both in the two-and three-nucleon system by considering not directly contact interactions between four nucleons, but to introduce auxiliary fields with the quantum numbers of the two-nucleon real and virtual bound states, coupling to two nucleons ², see e.g. [14, 15, 16]:

$$\begin{aligned} \mathcal{L}_{2N,t} = & -y \left[d_t^{i\dagger} (N^T P_t^i N) + \text{H.c.} \right] \\ & + d_t^{i\dagger} \left[\Delta_t - c_{0t} \left(i\partial_0 + \frac{\vec{\partial}^2}{4M} + \frac{\gamma_t^2}{M} \right) - \sum_{n=1}^{\infty} c_{nt} \left(i\partial_0 + \frac{\vec{\partial}^2}{4M} + \frac{\gamma_t^2}{M} \right)^{n+1} \right] d_t^i \end{aligned} \quad (2.1)$$

Here, $N = \binom{p}{n}$ is the nucleon iso-doublet and $P_t^i = \frac{1}{\sqrt{8}} \tau_2 \sigma_2 \sigma^i$ the projector onto the spin-triplet iso-spin-singlet state with vector index $i = 1, 2, 3$. σ^i (τ^A) are the spin (iso-spin) Pauli matrices, $A = 1, 2, 3$ the iso-vector indices. The auxiliary field d_t represents the deuteron with binding momentum $\gamma_t = \sqrt{MB_t} = 45.7025$ MeV. Strictly speaking, one should replace the (iso-scalar) nucleon mass $M \rightarrow M - B_t/2$ to obtain the correct deuteron mass, but this effect is negligible in what follows. Only the 3S_1 -channel of NN scattering is considered here; the 1S_0 -channel is discussed in Sect. 2.3. The choice of sign for c_{nt} is traditional [14].

That this Lagrangean is on-shell equivalent to the one containing only nucleon fields was formally shown in [15] by a Gauß'ian integration over d_t , followed by a field-redefinition and disregarding terms with more than four nucleon fields. The advantage of this scheme – stressed repeatedly [12, 15, 17] – is that the parameters follow naïve dimensional analysis: As again discussed in Sect. 2.2, $\Delta_t \sim Q$, with mass-dimension 1, is LO; the dimension-less parameter $c_{0t} \sim Q^0$ first appears at NLO since it comes with two powers of momentum, $c_{0t} \vec{p}^2 \sim Q^2$; while a dimension-full operator proportional to $c_{nt} \sim Q^0$ enters at N^{2n+1} LO because it is accompanied by $2n + 2$ powers of the typical momentum.

All interactions which are not pure S-wave – like SD-mixing, P-wave scattering between two nucleons etc. – are added either as interactions between the deuteron d_t and two nucleons, or between four nucleons [17, 16]. They are not listed as they are of higher order than necessary in the following – with the exception of SD mixing, whose effect will be neglected in the three-nucleon system, see the discussion in Sect. 3.1. The only additional term at N^2 LO is the kinetic energy of the nucleon, which up to relativistic corrections is:

$$\mathcal{L}_{1N} = N^\dagger \left(i\partial_0 + \frac{\vec{\partial}^2}{2M} \right) N \quad (2.2)$$

²As by-product, I attempt to unify the notational cornucopia of which the present author is not completely innocent. Throughout, the sub-script t (s) denotes quantities in the spin-triplet (singlet) channel of NN scattering.

The bare deuteron propagator i/Δ_t is thus dressed at LO by all interactions proportional to y with an arbitrary number of loops, see Fig. 1. At NLO, one perturbative insertion proportional to c_{0t} is included, followed by two at N²LO, and in general n at NⁿLO. In addition, one insertion of the operator proportional to c_{nt} enters at N²ⁿ⁺¹LO, etc.

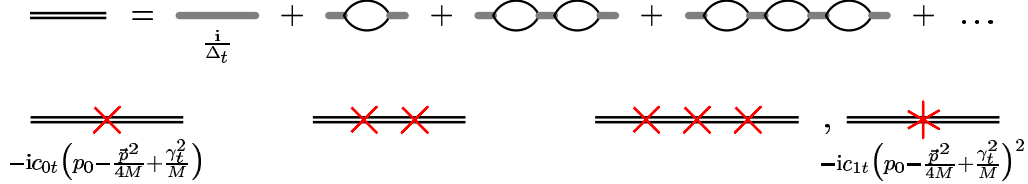


Figure 1: Top: Re-summation of the bare deuteron propagator (thick gray line) into the dressed deuteron propagator (double line) at LO by dressing with two-nucleon bubbles. Bottom: The NLO, N²LO and N³LO corrections to the deuteron propagator. The cross denotes an insertion of the deuteron kinetic-energy operator proportional to C_{0t} , the star one proportional to c_{1t} .

Choosing for the $d_t NN$ coupling constant without loss of generality

$$y^2 = \frac{4\pi}{M} , \quad (2.3)$$

the auxiliary-field propagator with kinetic energy p_0 and momentum \vec{p} becomes particularly simple in the low-energy expansion:

$$\begin{aligned} & i D_t(p_0, \vec{p}) \\ &= \frac{i}{\Delta_t + \mu - \sqrt{\frac{\vec{p}^2}{4} - Mp_0} - i\epsilon} \sum_{m=0}^{\infty} \left[\frac{c_{0t}(p_0 - \frac{\vec{p}^2}{4M} + \frac{\gamma_t^2}{M}) + \sum_{n=1}^{\infty} c_{nt} \left(p_0 - \frac{\vec{p}^2}{4M} + \frac{\gamma_t^2}{M} \right)^{n+1}}{\Delta_t + \mu - \sqrt{\frac{\vec{p}^2}{4} - Mp_0} - i\epsilon} \right]^m \\ &\rightarrow \frac{i}{\Delta_t + \mu - \sqrt{\frac{\vec{p}^2}{4} - Mp_0} - i\epsilon - c_{0t}(p_0 - \frac{\vec{p}^2}{4M} + \frac{\gamma_t^2}{M}) - \sum_{n=1}^{\infty} c_{nt} \left(p_0 - \frac{\vec{p}^2}{4M} + \frac{\gamma_t^2}{M} \right)^{n+1}} \end{aligned} \quad (2.4)$$

Here, μ is the regulator of the linear divergence in the nucleon loop, regularised using dimensional regularisation with the PDS subtraction scheme [18]. The scattering amplitude between two non-relativistic nucleons with relative centre-of-mass (cm) momentum k in the 3S_1 -channel is obtained by multiplying with $-y^2 = -4\pi/M$ and setting the nucleons on-shell

$(p_0 = k^2/M, \vec{p} = \vec{0})$:

$$\begin{aligned} \mathcal{A}_{NN}(k) &= -\frac{4\pi}{M} \frac{1}{\Delta_t + \mu + ik} \sum_{m=0}^{\infty} \left[\frac{c_{0t} \left(\frac{k^2}{M} + \frac{\gamma_t^2}{M} \right) + \sum_{n=1}^{\infty} c_{nt} \left(\frac{k^2}{M} + \frac{\gamma_t^2}{M} \right)^{n+1}}{\Delta_t + \mu + ik} \right]^m \\ &\rightarrow -\frac{4\pi}{M} \frac{1}{\Delta_t + \mu + ik - c_{0t} \left(\frac{k^2}{M} + \frac{\gamma_t^2}{M} \right) - \sum_{n=1}^{\infty} c_{nt} \left(\frac{k^2}{M} + \frac{\gamma_t^2}{M} \right)^{n+1}} \end{aligned} \quad (2.5)$$

To sum all effective-range corrections to all orders in the second line of (2.4) and (2.5) has no advantage but to shorten the following determination of the low-energy coefficients; actual calculations involve only a finite number of c_{nt} 's, in which case the difference between the two lines is formally of higher order. Problems with re-summing the effective-range corrections “to all orders” are discussed in Sect. 3.4.

2.2 ... with Z-Parameterisation

In Effective Range Expansion (ERE) around the deuteron pole [4], the scattering amplitude of two non-relativistic nucleons with relative cm momentum k in the 3S_1 -channel is

$$\mathcal{A}_{NN}({}^3S_1, k) = -\frac{M}{4\pi} \frac{1}{\gamma_t - \frac{\rho_{0t}}{2} (\gamma_t^2 + k^2) - \sum_{n=1}^{\infty} \rho_{nt} (\gamma_t^2 + k^2)^{n+1} + ik} , \quad (2.6)$$

where $\rho_{0t} = 1.764$ fm is the effective range, $\rho_{1t} = 0.389$ fm³ the shape parameter etc. Matching (2.5) to the ERE-result (2.6), one obtains the *ERE-parameterisation* of EFT(\not{p}):

$$\Delta_{t,ERE} + \mu_{ERE} = \gamma_t , \quad c_{0t,ERE} = \frac{\rho_{0t}}{2} M , \quad c_{nt,ERE} = \rho_{nt} M^{n+1} \quad \forall n \geq 1 \quad (2.7)$$

While γ_t is clearly a typical low-momentum scale in EFT(\not{p}), $\gamma_t \ll \Lambda_{\not{p}} \sim m_{\pi}$, the other parameters encode Physics beyond the breakdown scale and hence one expects $\rho_{nt} \sim \Lambda_{\not{p}}^{-2n-1}$ from dimensional analysis. Indeed, contributions to the scattering amplitude for example from the shape-parameter are small, with the expansion parameter Q estimated as $Q \sim \gamma_t \rho_{1t}^{1/3} \approx 0.17$. Therefore, the amplitude can be expanded in powers of $Q \sim \gamma_t^{1/(2n+1)} \rho_{nt}$, and an error estimate follows, rendering Effective Range Theory useful:

$$\mathcal{A}_{NN}({}^3S_1, k) = -\frac{M}{4\pi} \frac{1}{\gamma_t + ik} \left[1 + \frac{\rho_{0t}}{2} \frac{\gamma_t^2 + k^2}{\gamma_t + ik} + \left(\frac{\rho_{0t}}{2} \frac{\gamma_t^2 + k^2}{\gamma_t + ik} \right)^2 + \mathcal{O}(Q^3) \right] \quad (2.8)$$

A problem with the expanded version (2.8) arises however because the effective range is numerically somewhat larger than naively expected, $\rho_0 > m_{\pi}^{-1}$ or

$$\gamma_t \rho_{0t} \approx 0.41 . \quad (2.9)$$

While the deuteron binding energy is in ERE-parameterisation reproduced immediately at LO, the residue of the scattering amplitude at the deuteron pole is now only expanded in this numerically not-so-small parameter,

$$\begin{aligned}
\text{Res}[\mathcal{A}_{NN}(^3\text{S}_1, k = i\gamma_t)] &= -\frac{4\pi}{M} Z_t \quad \text{with} \\
Z_t &= \frac{1}{1 - \gamma_t \rho_{0t}} = 1.690(3) \\
&= 1 + \gamma_t \rho_{0t} + (\gamma_t \rho_{0t})^2 + (\gamma_t \rho_{0t})^3 + \dots = 1 + 0.409 + 0.167 + 0.068 + \dots ,
\end{aligned} \tag{2.10}$$

so that even including N²LO-effects, seven percent are missed to close the gap to the exact value. In contrast, not considering the N³LO shape-parameter effects in \mathcal{A} leads only to a deviation on the order of $\gamma_t^3 \rho_{1t} = 0.5\%$.

Clearly, the residue is an important characteristic of the two-body system as it determines the asymptotic normalisation of the deuteron wave-function at large distances r :

$$\Psi_{\text{deuteron}}(r \rightarrow \infty) = \sqrt{\frac{\gamma Z_t}{2\pi}} \frac{e^{-\gamma r}}{r} . \tag{2.11}$$

Phillips et al. [13] re-summed therefore the series in $\gamma_t \rho_{0t}$ partially by expressing ρ_{0t} via Z_t . To discuss its advantage, re-write (2.6) in a superficially more complicated way as

$$\begin{aligned}
&\frac{1 + (Z_t - 1)}{\gamma_t + ik} \frac{1}{1 + \frac{Z_t - 1}{2} \left(1 + \frac{ik}{\gamma_t}\right) - Z_t \sum_{n=1}^{\infty} \rho_{nt} (\gamma_t - ik) (\gamma_t^2 + k^2)^n} \\
&= \frac{1}{\gamma_t + ik} [1 + (Z_t - 1)] \left[1 - \frac{Z_t - 1}{2} \left(1 + \frac{ik}{\gamma_t}\right) + \left(\frac{Z_t - 1}{2} \left(1 + \frac{ik}{\gamma_t}\right)\right)^2 + \mathcal{O}(Q^3) \right] .
\end{aligned} \tag{2.12}$$

Formally, $Z_t - 1 \approx 0.69$ is still treated as a small expansion parameter in the resulting *Z-parameterisation*, but the deuteron residue is now restored already at NLO with no corrections from higher orders as the second denominator in (2.12) has no residue at $\gamma_t = -ik$:

$$Z_t = \underbrace{1}_{\text{LO}} + \underbrace{(Z_t - 1)}_{\text{NLO}} + \underbrace{0}_{\text{N}^n\text{LO}} , \quad n \geq 2 . \tag{2.13}$$

Outside the deuteron pole, the additional terms from Z_t also converge faster because the second term in the second denominator is a power series in $(Z_t - 1)/2 \approx 0.3$. A slight dis-advantage is that the expansion parameter for the higher-order correction is now bigger by 70%: $Z_t \rho_{nt} \gamma_t^{2n+1}$. Thus, the N³LO-correction from the shape parameter is now $\sim 0.8\%$. At this level of accuracy, however, other corrections (e.g. from P-wave interactions) must be considered, whose scale is also set by the pion mass and which are estimated to be stronger because $(\gamma_t / (\Lambda_\# \sim m_\pi))^3 \sim 3\%$.

In Z-parameterisation, the expanded version of the EFT(\not{p})-amplitude (2.5) is therefore first matched to reproduce the correct deuteron pole position: $\Delta_t + \mu = \gamma_t$. Then, the

residue is found starting at NLO as

$$Z_t \stackrel{!}{=} 1 + \sum_{n=1}^{\infty} \left(c_{0t} \frac{2\gamma_t}{M} \right)^n . \quad (2.14)$$

At LO, no additional free parameter exists in EFT and the residue is one. At higher orders, the residue is set equal to Z_t when c_{0t} is suitably chosen: With the expansion truncated at some finite order, $c_{0t} = \sum_{n=0}^{n_{\max}} c_{0t}^{(n)}$ contains now contributions from higher orders in the Q -expansion, $c_{0t}^{(n)}$ being $\mathcal{O}(Q^n)$. To summarise, the parameters in Z-parameterisation are

$$y^2 = \frac{4\pi}{M} \sim Q^0 \quad (2.15)$$

$$\Delta_t + \mu = \gamma_t \sim Q \quad (2.16)$$

$$c_{0t}^{(n)} = (-)^n (Z_t - 1)^{n+1} \frac{M}{2\gamma_t} \sim Q^n \quad (2.17)$$

$$c_{nt} = \rho_{nt} M^{n+1} \sim Q^0 \quad \forall n \geq 1 . \quad (2.18)$$

In contradistinction, c_{0t} receives in ERE-parameterisation only a contribution at order Q^0 , and none at higher orders (2.7). However, such an expansion is with our choice of Lagrangean (2.1) only encountered for one parameter, and not – as previously – for all [12, 15, 17, 19].

The auxiliary-field propagator to $N^2\text{LO}$,

$$D_t(p_0, \vec{p}) = \frac{1}{\gamma_t - \sqrt{\frac{\vec{p}^2}{4} - Mp_0 - i\epsilon}} \times \left[\underbrace{1}_{\text{LO}} + \underbrace{\frac{Z_t - 1}{2\gamma_t} \left(\gamma_t + \sqrt{\frac{\vec{p}^2}{4} - Mp_0 - i\epsilon} \right)}_{\text{NLO}} + \underbrace{\left(\frac{Z_t - 1}{2\gamma_t} \right)^2 \left(\frac{\vec{p}^2}{4} - Mp_0 - \gamma_t^2 \right)}_{\text{N}^2\text{LO}} + \mathcal{O}(Q^3) \right] , \quad (2.19)$$

is thus a faster-converging alternative to the usual ERE of the NN -scattering amplitude in the ${}^3\text{S}_1$ -channel. The wave-function renormalisation, i.e. the residue of the deuteron propagator, is by construction exact at NLO:

$$\mathcal{Z}_t := \left(\frac{\partial}{\partial p_0} \frac{1}{D_t(p_0, \vec{0})} \Big|_{p_0 = -\frac{\gamma_t^2}{M}} \right)^{-1} = \frac{2\gamma_t}{M} \left[\underbrace{1}_{\text{LO}} + \underbrace{(Z_t - 1)}_{\text{NLO}} + \underbrace{0}_{\text{N}^n\text{LO}} , n \geq 2 \right] \quad (2.20)$$

One could also replace directly the deuteron propagator in ERE by the result in Z-parameterisation (2.12), as e.g. argued to be computationally simpler by Beane and Savage [16]. This would be mandatory if $\gamma_t \rho_{0t} \approx 1$. Equivalently, if one re-sums all orders in c_{0t} , one finds again the ERE-parameterisation (2.7), $c_{0t} = \frac{Z_t - 1}{Z_t} \frac{M}{2\gamma_t} = \frac{\rho_{0t}}{2} M$. However, there are a number of dis-advantages of this approach, as will be discussed in Sect. 3.4.

2.3 Z-Parameterisation for the $^1\text{S}_0$ -channel?

The obvious question is: Why not also impose Z-parameterisation for the $^1\text{S}_0$ -channel of NN scattering? As its bound state is only virtual, one usually performs the ERE around zero momentum,

$$\mathcal{A}_{NN}(^1\text{S}_0, k) = -\frac{M}{4\pi} \frac{1}{-\frac{1}{a_s} - \frac{r_{0s}}{2} k^2 - \sum_{n=1}^{\infty} r_{ns} k^{2n+2} + i k} , \quad (2.21)$$

with $a_s = 23.714$ fm, $r_{0s} = 2.73$ fm, $r_{1s} = -0.48$ fm³ the scattering length, effective range and shape parameter. As $r_{0s}/a_s \approx 0.11$, the series-expansion of the residue of the virtual bound-state converges much faster than in the deuteron channel. Still, in order to simplify notation, consider a Lagrangean analogous to the $^3\text{S}_1$ -channel:

$$\begin{aligned} \mathcal{L}_{2N,s} = & -y \left(d_s^{A\dagger} (N^T P_s^A N) + \text{H.c.} \right) \\ & + d_s^{A\dagger} \left[\Delta_s - c_{0s} \left(i\partial_0 + \frac{\vec{\partial}^2}{4M} + \frac{\gamma_s^2}{M} \right) - \sum_{n=1}^{\infty} c_{ns} \left(i\partial_0 + \frac{\vec{\partial}^2}{4M} + \frac{\gamma_s^2}{M} \right)^{n+1} \right] d_s^A \end{aligned} \quad (2.22)$$

The auxiliary field d_s represents the spin-singlet iso-spin-triplet state, whose projector is $P_s^A = \frac{1}{\sqrt{8}} \sigma_2 \tau_2 \tau^A$. One now first re-writes the ERE expansion (2.21) in the form analogous to (2.6) in which the pole position does not change from order to order,

$$\mathcal{A}_{NN}(^1\text{S}_0, k) = -\frac{M}{4\pi} \frac{1}{\gamma_s - \frac{\rho_{0s}}{2} (\gamma_s^2 + k^2) - \sum_{n=1}^{\infty} \rho_{ns} (\gamma_s^2 + k^2)^{n+1} + i k} \quad (2.23)$$

and determines the coefficients by matching as

$$\gamma_s = \frac{1}{a_s} + \frac{r_{0s}}{2} \gamma_s^2 - \sum_{n=1}^{\infty} r_{ns} (-\gamma_s^2)^{n+1} \quad (2.24)$$

$$\rho_{0s} = r_{0s} + 2 \sum_{n=1}^{\infty} (n+1) r_{ns} (-\gamma_s^2)^n \quad (2.25)$$

$$\rho_{ms} = r_{ms} + \sum_{n=m}^{\infty} \binom{n+1}{m+1} r_{ns} (-\gamma_s^2)^{n-l} , \quad m > 0 . \quad (2.26)$$

Truncation at ρ_{0s} (ρ_{1s}) leads to the numerical values $\gamma_s = -7.8904$ MeV (-7.8902 MeV), $\rho_{0s} = 2.730$ fm (2.733 fm) (, $\rho_{1s} = r_{1s}$). The residue is indeed very close to unity:

$$Z_s = \frac{1}{1 - \gamma_s \rho_{0s}} = 0.9016 \text{ (0.9015)} \quad (2.27)$$

At N²LO, the difference between the perturbatively built residue $1 + \gamma_s \rho_{0s} + (\gamma_s \rho_{0s})^2 = 1 - 0.1092 + 0.0119 = 0.9027$ and the exact values is with 0.1% considerably smaller than

leaving out relativistic and other effects. In the results presented in the following Section, the difference between the ERE-parameterisation and Z-parameterisation for the 1S_0 -channel cannot be discerned in the plots of the phase-shifts. Still, the re-formulation serves the purpose to compactify and simplify formulae. The parameters of the Lagrangean are determined in Z-parameterisation by the analogue to (2.15):

$$y^2 = \frac{4\pi}{M} \sim Q^0 \quad (2.28)$$

$$\Delta_s + \mu = \gamma_s \sim Q \quad (2.29)$$

$$c_{0s}^{(n)} = (-)^n (Z_s - 1)^{n+1} \frac{M}{2\gamma_s} \sim Q^n \quad (2.30)$$

$$c_{ns} = \rho_{ns} M^{n+1} \sim Q^0 \quad \forall n \geq 1 \quad . \quad (2.31)$$

Note that in contradistinction to previous work, y is chosen to be identical in the spin-triplet and spin-singlet channel and thus carries no sub-script.

3 The Three-Body System in Z-Parameterisation

3.1 Formalism

With the parameters of the two-nucleon Lagrangean fixed by Z-parameterisation, it is now straight-forward to state the equations governing neutron-deuteron scattering. As they were derived repeatedly in the literature (see e.g. [17, 20, 21]), the following presentation focuses mainly on notation. Appendix A contains a brief overview, defining also the pertinent projection operators on the various partial waves and three-nucleon configurations.

Two cluster-configurations exist in the three-nucleon system: The Nd_t -cluster with total spin $S = \frac{3}{2}$ or $S = \frac{1}{2}$, depending on whether the deuteron and nucleon spins are parallel or anti-parallel; and the Nd_s -cluster which has total spin $S = \frac{1}{2}$, as d_s^A is a scalar. The leading-order three-particle amplitude is $\mathcal{O}(Q^{-2})$ (before wave-function renormalisation) and includes all diagrams built out of the leading two-body interactions, i.e. the ones proportional to y and Δ_t , Δ_s in the two-nucleon Lagrangeans (2.1/2.22). The resultant Faddeev integral equation – first derived by Skorniakov and Ter-Martirosian [20] without three-body force – is pictorially represented in Fig. 2.

As the Lagrangean up to N²LO does not mix partial waves or flip the spin of the auxiliary fields, angular momentum is conserved in the quartet and doublet channels. Strictly speaking, SD-mixing in the deuteron channel produces a splitting and mixing of the three-body amplitudes with the same spin and angular momentum but different total angular momentum. However, we limit ourselves to the averaged phase-shifts, as the splitting is not going to be realistic enough to describe spin-observables in the three-nucleon system. This path was also pursued in [12] and [17] which used ERE-parameterisation, to which the findings in Z-parameterisation will be compared. An analysis of these splitting is postponed to a future presentation, which also deals with spin-observables in the three-nucleon system.

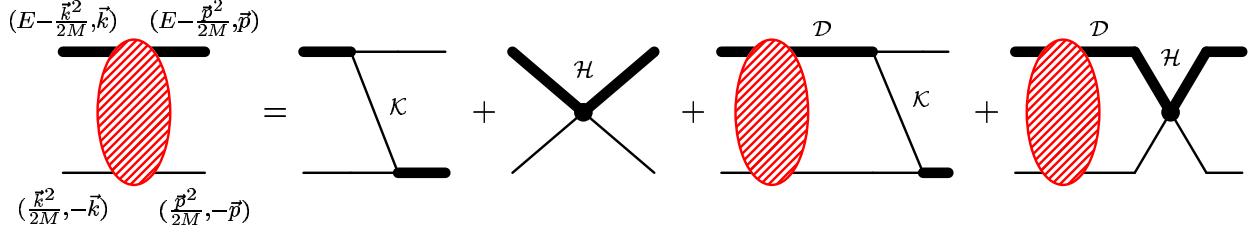


Figure 2: The Faddeev equation for Nd -scattering to $N^2\text{LO}$. Thick solid line: propagator of the two intermediate auxiliary fields d_s and d_t , denoted by \mathcal{D} , see (3.6); \mathcal{K} : propagator of the exchanged nucleon, see (3.2); \mathcal{H} : three-body force, see (3.11).

The spin-quartet channel of the Nd -system is particularly simple. The l th partial wave of the amplitude $t_q^{(l)}$ in the centre-of-mass (cm) frame is given by³

$$t_q^{(l)}(E; k, p) = -4\pi \mathcal{K}^{(l)}(E; k, p) + \frac{2}{\pi} \int_0^\infty dq q^2 \mathcal{K}^{(l)}(E; q, p) D_t(E - \frac{q^2}{2M}, q) t_q^{(l)}(E; k, q) . \quad (3.1)$$

The total non-relativistic energy is $E := \frac{3\vec{k}^2}{4M} - \frac{\gamma^2}{M}$; the incoming (outgoing) deuteron-momentum \vec{k} (\vec{p}); and the projected propagator of the exchanged nucleon on angular momentum l ⁴

$$\mathcal{K}^{(l)}(E; q, p) := \frac{1}{2} \int_{-1}^1 dx \frac{P_l(x)}{p^2 + q^2 - ME - i\epsilon + pqx} = \frac{(-1)^l}{pq} Q_l \left(\frac{p^2 + q^2 - ME - i\epsilon}{pq} \right) , \quad (3.2)$$

where the l th Legendre polynomial of the second kind with complex argument is as in [22]

$$Q_l(z) = \frac{1}{2} \int_{-1}^1 dt \frac{P_l(t)}{z - t} . \quad (3.3)$$

In the doublet channel, the Faddeev equation is two-dimensional in cluster-configuration space as both Nd_t - and Nd_s -configurations contribute:

$$\begin{aligned} \vec{t}_d^{(l)}(E; k, p) &= 2\pi \left[\mathcal{K}^{(l)}(E; k, p) \begin{pmatrix} 1 \\ -3 \end{pmatrix} + \delta^{l0} \mathcal{H}(E; \Lambda) \begin{pmatrix} 1 \\ -1 \end{pmatrix} \right] \\ &\quad - \frac{1}{\pi} \int_0^\infty dq q^2 \left[\mathcal{K}^{(l)}(E; q, p) \begin{pmatrix} 1 & -3 \\ -3 & 1 \end{pmatrix} + \delta^{l0} \mathcal{H}(E; \Lambda) \begin{pmatrix} 1 & -1 \\ -1 & 1 \end{pmatrix} \right] \\ &\quad \times \mathcal{D}(E - \frac{q^2}{2M}, q) \vec{t}_d^{(l)}(E; k, q) \end{aligned} \quad (3.4)$$

³The sub-script q (d) denotes quantities in the spin-quartet (doublet) channel of the three-nucleon system.

⁴This corrects a typographical error in a previous paper on the higher partial waves in the Nd -system [17], affecting the odd partial waves.

The three-body force \mathcal{H} will be discussed in the next Sub-section. The vector

$$\vec{t}_d^{(l)} := \begin{pmatrix} t_{d,tt}^{(l)} \\ t_{d,ts}^{(l)} \end{pmatrix} \quad (3.5)$$

is built out of the two amplitudes which get mixed: $t_{d,tt}^{(l)}$ for the $Nd_t \rightarrow Nd_t$ -process, and $t_{d,ts}^{(l)}$ for the $Nd_t \rightarrow Nd_s$ -process. Furthermore,

$$\mathcal{D}(p_0, p) := \begin{pmatrix} D_t(p_0, p) & 0 \\ 0 & D_s(p_0, p) \end{pmatrix} \quad (3.6)$$

is the propagator of the two intermediate auxiliary fields.

How to calculate higher-order corrections? The re-summation of all interactions proportional to y and $\Delta_{s/t}$ into a Faddeev equation is mandatory since the power-counting classifies all diagrams which are built only out of them as contributing equally strong to the final amplitude. Ref. [12] proposed to calculate the higher-order corrections by expanding the kernel and inhomogeneous part of the integral equation in powers of Q to the desired order of accuracy, and iterate then by inserting it into a Faddeev equation (*partially re-summed $N^n LO$ -calculation*). This re-summation of some higher-order effects does not increase the accuracy of the calculation, which is still set by the accuracy to which the kernel is expanded. It does however simplify the numerical treatment, as no divergences in the amplitude or in three-body forces \mathcal{H} are encountered as the numeric cut-off is removed. It also leads to a simple, analytical argument at which orders three-body forces with derivatives enter, as discussed below. In contradistinction, a *strict perturbation* around the LO solution soon becomes cumbersome numerically, as full off-shell amplitudes need to be computed and the numerical integrals soon start to diverge, making a numerical renormalisation necessary [32].

The computational effort to solve the integral equations (3.1/3.4) numerically is trivial, as all potentials are separable. A simple Mathematica-code can be down-loaded from <http://www.physik.tu-muenchen.de/~hgrie>. Here, a step-function cut-off Λ in momentum space was chosen. The cut-off dependence of the results is discussed below. To reduce the numerical instabilities from the poles of the two-nucleon amplitudes and logarithmic singularities of the projected nucleon propagator in the kernel, the integral equations are – following Hetherington and Schick [33] – first solved on a contour in the complex plane. The amplitudes on the real axis are then re-constructed by another use of the equations. A grid of 70 points does more than suffice for numerical stability. For example, the imaginary parts of $k \cot \delta$ vanish below the deuteron-dis-integration threshold easily to 1 part in 10^8 .

Finally, the scattering phase-shift of the l th partial wave in the quartet and doublet channel is related to the renormalised on-shell amplitudes by

$$T_q^{(l)} = \mathcal{Z}_t \, t_q^{(l)} = \frac{3\pi}{M} \frac{1}{k \cot \delta_q^{(l)} - ik} , \quad T_{d,xy}^{(l)} = \frac{3\pi}{M} \frac{1}{k \cot \delta_{d,xy}^{(l)} - ik} . \quad (3.7)$$

where $x, y = s, t$ label the matrix entries in cluster-configuration space, and

$$\vec{T}_d^{(l)} = \mathcal{Z} \vec{t}_d^{(l)} \quad \text{with} \quad \mathcal{Z} := \begin{pmatrix} \mathcal{Z}_t & 0 \\ 0 & \sqrt{\mathcal{Z}_t \mathcal{Z}_s} \end{pmatrix} \quad (3.8)$$

is the renormalised doublet-amplitude and its wave-function renormalisation. In the doublet channel, the only observable process is nucleon-deuteron scattering, $Nd_t \rightarrow Nd_t$, i.e. $x = y = t$. Results are not discussed for the un-physical processes $Nd_t \leftrightarrow Nd_s$ and $Nd_s \rightarrow Nd_s$.

The elastic differential cross-section from Nd -scattering in the cm-frame is finally [34]

$$\frac{d\sigma}{d\Omega} = \frac{1}{3} \left[\left| \sum_{l=0}^{\infty} (2l+1) \frac{P_l(\cos \theta)}{k \cot \delta_{d,tt} - ik} \right|^2 + 2 \left| \sum_{l=0}^{\infty} (2l+1) \frac{P_l(\cos \theta)}{k \cot \delta_q - ik} \right|^2 \right]. \quad (3.9)$$

A maximum angular momentum $l_{\max} = 4$ serves to converge the differential cross-section.

The recipe to compute Nd -scattering up to $N^2\text{LO}$ is hence as follows: Expand the auxiliary-field propagators and their wave-function renormalisations in the integral equations (3.1/3.4) to the desired level of accuracy in Z-parameterisation as in (2.19/2.20), and then solve the Faddeev equation. To $N^2\text{LO}$, the projected nucleon propagator $\mathcal{K}^{(l)}$ is unchanged.

Nucleon-deuteron scattering is to $N^2\text{LO}$ thus completely determined by four simple observables of NN -scattering: the deuteron binding energy and residue (or effective range), and the scattering length and effective range of the $^1\text{S}_0$ -channel. Only the $^2\text{S}_1$ -channel has further unknowns, namely the strength of the three-body interaction H_0 at LO and NLO , and in addition of H_2 at $N^2\text{LO}$, as discussed momentarily. They are determined by its measured scattering length a_d [31] and the triton binding energy B_d , respectively:

$$a_d = (0.65 \pm 0.04) \text{ fm} , \quad B_d = 8.48 \text{ MeV} \quad (3.10)$$

But why are two and only two three-body force needed at $N^2\text{LO}$?

3.2 Three-body Force and Lagrangean

We now turn to the three-body force \mathcal{H} already included in the doublet-channel Faddeev equation (3.4). The Pauli principle in the quartet channel and the centrifugal barrier in all partial waves $l > 0$ forbids three-body forces in nearly all partial waves at $N^2\text{LO}$; see also [23]. However, neither rules out a three-body force without derivatives in the $^2\text{S}_{\frac{1}{2}}$ -wave, the physically most interesting channel, which contains the triton and ^3He as real bound states. While one would naïvely have guessed that such an energy-independent three-body force scales as Q^0 and hence enters only at $N^2\text{LO}$, an unusual renormalisation of the three-nucleon system in the triton channel mandates its inclusion into the Faddeev equation as a LO term: As was first pointed out by Minlos and Faddeev [25], this channel suffers from a peculiar cut-off sensitivity of the on-shell amplitudes if three-body forces are absent. The kernel of (3.4) is for $l = 0$ at short distances identical to the one of an attractive $1/r^2$ -potential between the auxiliary fields and the nucleon [10]. Without a three-body force, the wave function would hence collapse, and all observables would become sensitive to Physics at very short distances, a phenomenon well-known as Thomas effect [24]. Its mathematical origin lies in the fact that in the absence of a three-body force, the solution to the integral equation is not unique because it allows for a zero mode, as the kernel of the doublet-S wave Faddeev equation is not compact [26].

In praxi, the integral equation is solved numerically by imposing a cut-off Λ , which should not be confused with the breakdown-scale Λ_{\neq} of $\text{EFT}(\neq)$. In that case, a unique solution exists in the $^2\text{S}_{\frac{1}{2}}$ -channel for each Λ and $\mathcal{H} = 0$, but no unique limit as $\Lambda \rightarrow \infty$. The Nd -scattering length, for example, can be tuned as a function of Λ to have any value between minus infinity and plus infinity. As long-distance phenomena must however be insensitive to details of the short-distance Physics (and in particular of the regulator chosen), Bedaque et al. [12, 21, 27] showed that the system must be stabilised by a three-body force

$$\mathcal{H}(E; \Lambda) = \frac{2}{\Lambda^2} \sum_{n=0}^{\infty} H_{2n}(\Lambda) \left(\frac{ME + \gamma_t^2}{\Lambda^2} \right)^n = \frac{2H_0(\Lambda)}{\Lambda^2} + \frac{2H_2(\Lambda)}{\Lambda^4} (ME + \gamma_t^2) + \dots \quad (3.11)$$

which absorbs all dependence on the cut-off as $\Lambda \rightarrow \infty$. It is analytical in E and can be obtained from a three-body Lagrangean, employing a three-nucleon auxiliary field analogous to the treatment of the two-nucleon channels, see [12] and the end of this Sub-Section.

H_{2n} is dimension-less but depends on the cut-off Λ in a non-trivial way, as a renormalisation-group analysis reveals: Instead of approaching a fixed-point as $\Lambda \rightarrow \infty$, it shows an oscillatory behaviour known as “limit cycle” [27, 28, 29].

As one needs a three-body force at LO, $H_0 \sim Q^{-2}$, to prevent the system from collapse, all three-body forces obtained by expanding \mathcal{H} in powers of E are also enhanced, with the interactions proportional to H_{2n} entering at $N^{2n}\text{LO}$ [12]. Since a numerical verification of this analytical observation is one of the prime advantages Z-parameterisation has, the argument is recalled here: Building the linear combination

$$\vec{t}_{\text{Wigner}}^{(0)} := \begin{pmatrix} t_{\text{Wigner},-}^{(0)} \\ t_{\text{Wigner},+}^{(0)} \end{pmatrix} = \frac{1}{2} \begin{pmatrix} 1 & -1 \\ 1 & 1 \end{pmatrix} \begin{pmatrix} t_{d,tt}^{(0)} \\ t_{d,ts}^{(0)} \end{pmatrix}, \quad (3.12)$$

the Faddeev equation becomes in the $^2\text{S}_{\frac{1}{2}}$ -channel

$$\begin{aligned} \vec{t}_{\text{Wigner}}^{(0)}(E; k, p) &= 4\pi \left[\mathcal{K}^{(0)}(E; k, p) \begin{pmatrix} 1 \\ -\frac{1}{2} \end{pmatrix} + \mathcal{H}(E; \Lambda) \begin{pmatrix} \frac{1}{2} \\ 0 \end{pmatrix} \right] \\ &\quad - \frac{2}{\pi} \int_0^\infty dq q^2 \begin{pmatrix} 2\mathcal{K}^{(0)}(E; q, p) + \mathcal{H}(E; \Lambda) & 0 \\ 0 & -\mathcal{K}^{(0)}(E; q, p) \end{pmatrix} \\ &\quad \times \begin{pmatrix} \Sigma(E - \frac{q^2}{2M}, q) & \Delta(E - \frac{q^2}{2M}, q) \\ \Delta(E - \frac{q^2}{2M}, q) & \Sigma(E - \frac{q^2}{2M}, q) \end{pmatrix} \vec{t}_{\text{Wigner}}^{(0)}(E; k, q) . \end{aligned} \quad (3.13)$$

While $\Sigma := \frac{1}{2}(D_t + D_s) = \frac{1}{2}\text{tr}\mathcal{D}$ is the “average” NN -S-wave scattering amplitude, $\Delta := \frac{1}{2}(D_t - D_s) = \frac{1}{2}\text{str}\mathcal{D}$ parameterises the degree to which the $^3\text{S}_1$ - and $^1\text{S}_0$ -channel differ. In the Wigner- $SU(4)$ -limit of arbitrary combined spin- and iso-spin rotation [30], the two amplitudes are identical, $\gamma_t = \gamma_s$, $\rho_{nt} = \rho_{ns} \forall n$. In that case, $\Delta = 0$, and the two equations for $t_{\text{Wigner},\neq}^{(0)}$ decouple. The essential observation is now that for the UV-behaviour of the amplitude, in which all scales are discarded except for the off-shell momentum $q \sim \Lambda$ in the

loop, the Wigner- $SU(4)$ -limit is recovered automatically. $t_{\text{Wigner},+}^{(0)}$ obeys the same integral equation as the quartet-S-wave in (3.1), where the Pauli principle forbids three-body forces without derivatives. Only $t_{\text{Wigner},-}^{(0)}$ is subject to the Wigner- $SU(4)$ symmetric three-body force \mathcal{H} . Its integral equation is the same as for three spin-less bosons, whose wave-function is well-known to collapse in the absence of three-body forces [25, 26, 27]. H_0 therefore must be LO to ensure that the physical on-shell amplitude is cut-off independent.

To determine the running of H_2 , one expands the quantities of (3.13) for $q \gg k, p, \gamma, \dots$:

$$\begin{aligned}
& \text{LO} & \text{NLO} & \text{N}^2\text{LO} \\
\Sigma(E - \frac{q^2}{2M}, q) & \rightarrow -\sqrt{\frac{4}{3}} \frac{1}{q} & -\frac{4\gamma}{3q^2} - \frac{Z-1}{2\gamma} & -\frac{4ME + 8\gamma^2}{3\sqrt{3}q^3} - \sqrt{\frac{4}{3}} \frac{Z-1}{q} - \frac{\sqrt{3}(Z-1)^2}{8\gamma^2} q + \dots \\
\mathcal{K}^{(0)}(E; q, p) & \rightarrow \frac{1}{q^2} & & + \frac{ME - \frac{2q^2}{3}}{q^4} + \dots \\
\implies \mathcal{H}(E; \Lambda) & \rightarrow \frac{2H_0^{\text{LO}}(\Lambda)}{\Lambda^2} + \frac{2H_0^{\text{NLO}}(\Lambda)}{\Lambda^2} & + \frac{2H_0^{\text{N}^2\text{LO}}(\Lambda)}{\Lambda^2} + \frac{ME + \gamma^2}{\Lambda^2} \frac{2H_2(\Lambda)}{\Lambda^2} + \dots
\end{aligned} \tag{3.14}$$

At LO, H_0 is independent of two-body observables and is fixed by a three-body datum. At NLO, only Σ has non-vanishing contributions. They depend only on the low-energy two-body observables $\gamma \sim Q$ and $\rho_0 \sim Q^0$, but not on the total cm-energy $E \sim Q^2$ – or equivalently, not on the on-shell momentum $k \sim Q$. The cut-off dependence they induce can hence be absorbed by $H_0^{\text{NLO}}(\Lambda)$, a momentum-independent correction to the LO three-body force whose value now depends also on the two-body observables γ and ρ_0 .

At N^2LO , more corrections arise which depend on γ and ρ_0 . In addition, both the projected nucleon propagator \mathcal{K} and the NN -scattering amplitude Σ show corrections proportional to ME . To match the behaviour of the off-shell (UV-)amplitude on the physical on-shell momentum E , the inclusion of an *energy-dependent* three-body force H_2 is thus mandatory. Its value is not determined by two-body observables. The expansion in powers of $E \sim Q^2$ proceeds straightforwardly: Another three-body force $H_{2n}(\Lambda)$ proportional to E^n is needed every even order in Q from expanding both Σ and $\mathcal{K}^{(0)}$. $H_{2n}(\Lambda)$ first enters at N^{2n}LO , independent of two-body observables. To determine its strength, one additional three-body datum is needed. The power-counting for the three-body forces is hence

$$H_0 \sim Q^{-2}, \quad H_2 \sim Q^{-2}, \quad H_{2n} \sim Q^{-2}. \tag{3.15}$$

Corrections to the limit $q \rightarrow \infty$ from the breaking of Wigner- $SU(4)$ -symmetry can only induce a momentum-dependent three-body force, because the only three-body force without derivatives is necessarily Wigner- $SU(4)$ -symmetric [21]. They can be shown to be of higher order, see [12] for a more detailed discussion.

The chain of isotropic (S-wave) Wigner- $SU(4)$ -symmetric three-body forces is also found from a three-nucleon auxiliary-field Lagrangean, incomplete analogy to the treatment of the

two-nucleon auxiliary fields in Sects. 2.1/2.3 [12, 21]:

$$\begin{aligned}\mathcal{L}_{3N} = & -\frac{y_3(\Lambda)}{\sqrt{3}} \left[t^\dagger \left((\sigma^i N) d_t^i - (\tau^A N) d_s^A \right) + \text{H.c.} \right] \\ & + t^\dagger \left[\Omega - \sum_{n=1}^{\infty} h_{2n}(\Lambda) \left(i\partial_0 + \frac{\vec{\partial}^2}{6M} + \frac{\gamma_t^2}{M} \right)^n \right] t ,\end{aligned}\quad (3.16)$$

where the auxiliary field t has the quantum numbers of the triton/ ${}^3\text{He}$, i.e. spin and isospin $\frac{1}{2}$. The relative coupling strength between the processes $t \rightarrow Nd_t$ and $t \rightarrow Nd_s$ is fixed because there is only one three-body force without derivatives, which also happens to be Wigner- $SU(4)$ -symmetric [12, 21]. This field is treated analogously to the two-nucleon auxiliary fields: At LO, the propagator of a ‘‘triton’’ with kinetic energy E and momentum \vec{p} is proportional to $\frac{1}{\Omega}$, with insertions proportional to $h_{2n}(\Lambda)$ suppressed by n powers of the triton kinetic energy:

$$\frac{i}{\Omega} \left[1 + \frac{h_2(\Lambda)}{M\Omega} \left(ME - \frac{\vec{p}^2}{6} + \gamma_t^2 \right) + \dots \right] \quad (3.17)$$

Comparing the final result of the resultant three-body force in the ${}^2\text{S}_{\frac{1}{2}}$ -wave (A.13) with (3.4), one finds that the couplings $y_3(\Lambda)$ and $h_{2n}(\Lambda)$ are in the cm-frame related to \mathcal{H} by

$$\mathcal{H}(E; \Lambda) = -\frac{2y_3^2(\Lambda)}{y^2 M\Omega} \left[1 + \sum_{m,n=1}^{\infty} \left[\frac{h_{2n}(\Lambda)}{\Omega M^n} (ME + \gamma_t^2)^n \right]^m \right] \quad (3.18)$$

or matching order by order the dimension-less three-body strengthes $H_{2n}(\Lambda)$ of (3.11),

$$H_0(\Lambda) = -\frac{y_3^2(\Lambda)}{y^2} \frac{\Lambda^2}{M\Omega} , \quad H_2(\Lambda) = -\frac{y_3^2(\Lambda)}{y^2} \frac{\Lambda^4}{(M\Omega)^2} h_2(\Lambda) , \dots , \quad (3.19)$$

so that the couplings are particularly simple when one chooses

$$\Omega = \frac{\Lambda^2}{M} , \quad y_3^2(\Lambda) = -y^2 H_0(\Lambda) , \quad h_2(\Lambda) = \frac{H_2(\Lambda)}{H_0(\Lambda)} , \quad (3.20)$$

as they follow then from (3.15) the natural scaling laws – with the exception of $y_3(\Lambda)$:

$$y_3^2(\Lambda) \sim Q^{-2} , \quad \Omega \sim Q^0 , \quad h_{2n}(\Lambda) \sim Q^0 \quad (3.21)$$

Notice that in contradistinction to $D_{s/t}$ in Sect. 2.1, the power counting does not require even a partial re-summation of the triton propagator.

3.3 The ${}^2\text{S}_{\frac{1}{2}}$ - (Triton-) Channel

That Z-parameterisation improves convergence is most importantly seen in the only channel in which a bound state is found, and in which the three-body force enters already at LO to

stabilise the system from collapse. In particular, it can be instrumentalised to confirm that the first momentum-dependent three-body force enters at N^2LO , as the analytical argument of the preceding section demands.

Previously, Hammer and Mehen calculated the $^2S_{\frac{1}{2}}$ -wave phase shifts below the deuteron break-up to NLO by sandwiching the ERE-corrections to the two-particle propagators between the LO half off-shell amplitudes [32]. ERE-parameterisation was also used in the recent article which proposed partially re-summed N^nLO -calculations to simplify numerics and showed that the momentum-dependent three-body force H_2 is conceptually necessary at N^2LO [12]. An estimate of NLO -effects in Z -parameterisation by Afman and Phillips [35] included the part of the two-particle propagator (2.19/2.20) which leads to the correct residues $Z_{s/t}$, but not the part which changes the off-shell propagation of the deuteron field, iterating again the perturbatively expanded kernel.

In the following, one has to differentiate between two kinds of convergence: First, the results should of course agree with available measurements, at the level of accuracy predicted by EFT. Second, it is vital for a reliable error-estimate and hence for predicting the accuracy of the calculation that EFT can demonstrate that contributions which are classified as higher-order are indeed suppressed, i.e. that corrections from order to order become smaller in the range of validity. In particular whenever no or scarce data are available, this *a-priori* error-estimate is essential to minimise the theoretical bias in the description of few-body properties. Z -parameterisation improves both variants over ERE-parameterisation.

The ERE- and Z -parameterisation results for the phase-shifts of the $^2S_{\frac{1}{2}}$ -channel at LO , NLO and N^2LO are shown in Fig. 3, together with the only available phase-shift analysis [36], dating from 1967, and results using the Argonne V18 potential supplemented with the Urbana IX three-body force [37, 38]. At this order, considerably more sophisticated and involved potential-model calculations must agree with the EFT-predictions, if all are fitted to the same low-energy observables. For lack of a direct phase-shift analysis of the three-nucleon system, convergence to experiment is discussed by comparison to such a potential-model calculation which reproduces the same two-nucleon observables, triton binding energy and scattering length in the $^2S_{\frac{1}{2}}$ -wave. At higher orders, EFT-calculations may be more accurate than those of potential models, because the EFT-result will depend on new three-body low-energy coefficients which do *not* enter in potential models, while a systematic treatment of three-body forces is built into EFT($\not\!f$).

At LO , both parameterisations are identical. As expected from the discussion in Sect. 2.2, the NLO corrections are larger for Z -parameterisation than for the ERE-version due to the inclusion of the full strength of the deuteron residue. Higher-order corrections in Z -parameterisation should be considerably smaller than in ERE-parameterisation, because their typical scale from NN -scattering is in the former set by $(Z_t - 1)/2 \approx 0.3$, while in the latter, it is $\gamma_t \rho_{0t} \approx 0.4$. This amounts to a difference in the predicted accuracy of the N^2LO -calculation of $(0.3)^3 \approx 3\%$ in Z -parameterisation versus $(0.4)^3 \approx 6.5\%$ in ERE-parameterisation for typical momenta in the three-body problem. Indeed, the correction from NLO to N^2LO is in general larger for the ERE-parameterisation than for the Z -parameterisation, and the result closer to the potential-model values. The plot of the logarithmic deviation of the on-shell point of the inverse K -matrix, $k \cot \delta$, from the

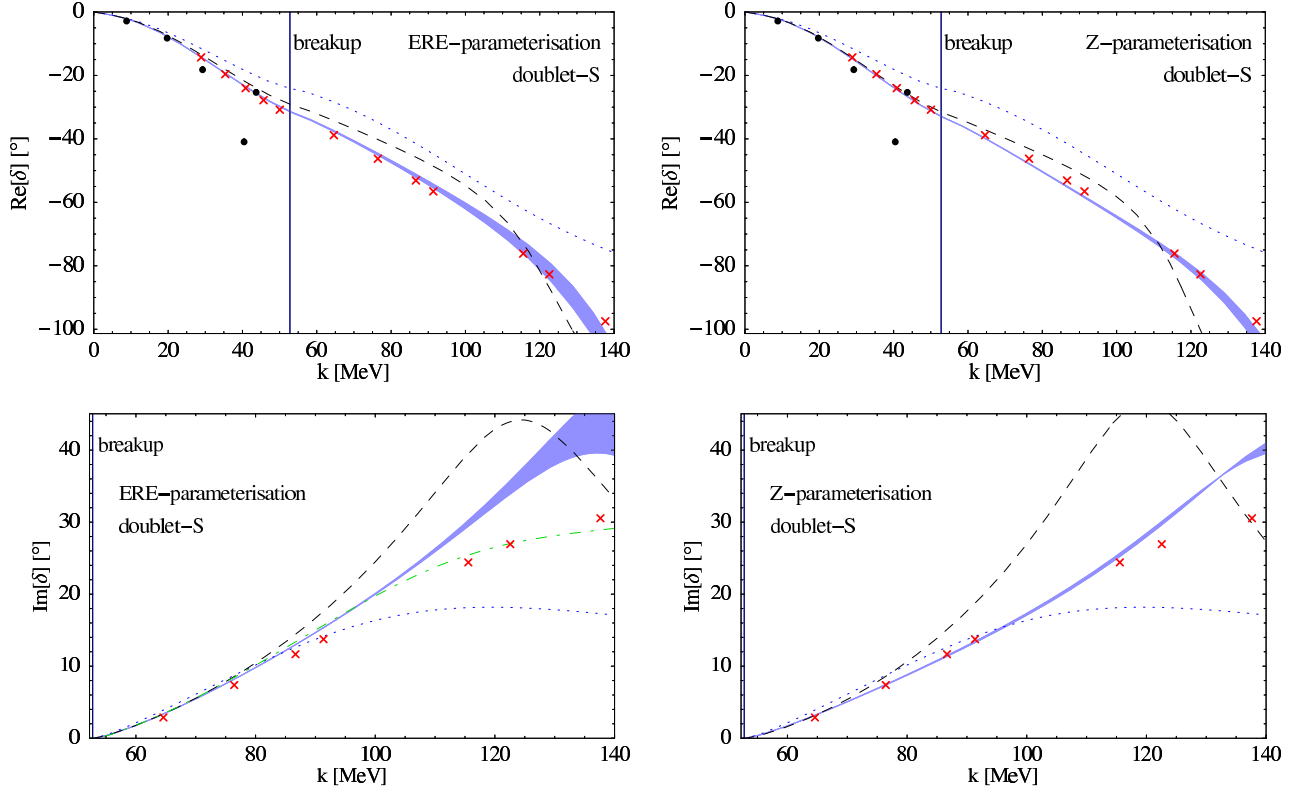


Figure 3: Comparison of the real (top) and imaginary (bottom) parts of the neutron-deuteron $^2S_{\frac{1}{2}}$ -phase-shift at LO (dotted), NLO (dashed) and N²LO (dark band) in ERE-parameterisation (left) and Z-parameterisation (right) as function of the cm-momentum k . The band in the N²LO-curve shows the variation induced by shifting the cut-off from $\Lambda = 200$ MeV to ∞ . Dots: phase-shift analysis from 1967 [36]; crosses: Argonne V18 results including the Urbana IX three-body force from [37] below, and from [38] above break-up. At LO and NLO, the results for $\Lambda = 1000$ MeV are shown. The dot-dashed curve in the imaginary parts of the ERE-result is a partial N³LO-calculation as described in the text.

potential-model numbers at each order in both parameterisations verifies these findings on the quantitative level, see left panel in Fig. 4.

In particular, the ERE-result for the imaginary part of the phase-shift has at large momenta not converged to the potential-model results at N²LO, while Z-parameterisation agrees with these data. As the effective-range effects are expected to be the dominant corrections in ERE-parameterisation, the imaginary part of the ERE-result in Fig. 3 contains also a computation in which these are included in the deuteron propagator (2.4) to order $(\gamma_t \rho_{0t})^3$. This is only a partial N³LO-calculation, neglecting shape-parameter, relativistic, SD-mixing and other corrections, but improves the agreement to the level achieved already at N²LO in Z-parameterisation. Close to $k = m_\pi \approx \Lambda_\pi$, both parameterisations become

un-reliable as the NLO and N²LO-corrections are comparable in size.

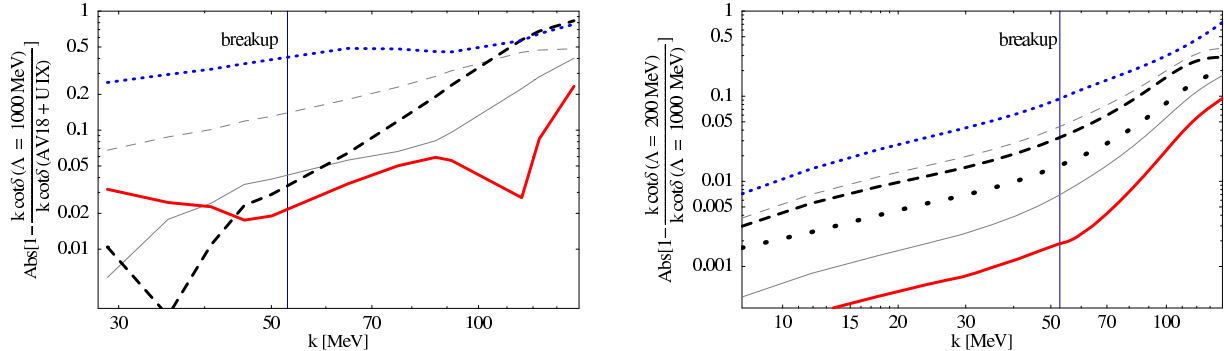


Figure 4: Convergence of $k \cot \delta$ as function of the cm momentum. Left: deviation from the result of the potential-model calculation [37, 38]. Right: dependence on cut-off variations between $\Lambda = 200$ and 1000 MeV. Dotted: LO; dashed: NLO; solid: N²LO; thin lines: ERE-parameterisation; thick lines: Z-parameterisation. Thick dots on the right: “N²LO”-calculation in Z-parameterisation with H_2 set to zero.

At least as important is that the internal convergence is drastically improved in Z-parameterisation. This is evident from the right side of Fig. 4 which compares the uncertainties induced into the N²LO phase-shifts by cut-off variations. As outlined in the Introduction, the main strength of the EFT-approach is that it allows for an *a-priori* estimate of the theoretical uncertainties of a calculation because contributions to the amplitudes are ordered by a small expansion parameter Q . NⁿLO corrections to $k \cot \delta$ should typically be of the order

$$\Delta(k \cot \delta) \sim Q^n = \left(\frac{p_{\text{typ}}}{\Lambda_{\text{f}}} \right)^n \quad (3.22)$$

compared to the LO result. Typical low-momentum scales p_{typ} in the three-body system are the binding momenta of the two-nucleon real and virtual bound states, $\gamma_s \approx -8.0$ MeV, $\gamma_t \approx 45$ MeV and the scattering momentum k . In addition, the three-body forces are determined in part by the typical three-nucleon bound-state momentum $\gamma_d = \sqrt{MB_d} \approx 90$ MeV. The breakdown scale $\Lambda_{\text{f}} \approx m_\pi$ of the theory is the scale at which higher-order corrections become comparable in size. Like the actual size of the expansion parameter Q , its value must be verified in actual calculations.

As observables at low energies must be independent of details of short-distance physics, they must be independent of the arbitrary regulator Λ up to the order of the expansion. In other words, the physical scattering amplitude (or more accurately its physically relevant part, $k \cot \delta$) must be dominated by integrations over off-shell momenta q in the integral equations (3.1/3.4) in the region in which the EFT is applicable, $q \lesssim \Lambda_{\text{f}}$. As argued e.g. by Lepage [39], one can therefore estimate sensitivity to short-distance Physics, and hence provide a reasonable error analysis, by varying the cut-off Λ between the break-down scale

Λ_{\neq} and ∞ . *In praxi*, an upper limit $\Lambda_{\max} = 1000$ MeV suffices since the phase-shifts are essentially cut-off independent beyond $\Lambda \approx 600$ MeV.

On the right in Fig. 4, the logarithmic cut-off variation is displayed as function of the cm momentum, both for ERE- and Z-parameterisation. Several points are worth noticing.

First, the cut-off variation is substantially smaller in Z-parameterisation over the whole range. For example, at the typical three-body scale $k \sim \sqrt{MB_d} \approx 90$ MeV, the cut-off variation is decreased from 15% and 4% at NLO and $N^2\text{LO}$ in ERE-parameterisation to 12% and 1.3% in Z-parameterisation⁵.

With k the dominant low-energy scale for momenta above the breakup point $(4\gamma_t^2/3)^{1/2} \approx 52$ MeV, one can secondly verify the estimate (3.22) for the corrections by fitting n to the nearly straight lines in the right panel of Fig. 4 in the momentum range between 70 and 100 to 130 MeV. At lower momenta, the slope does not change significantly from order to order because the dominant corrections are $\sim (\gamma_{s,t}/\Lambda)^n$ and hence nearly independent of k . The power-law obtained for each order and parameterisation is listed in Table 1. The slope increases in Z-parameterisation by one unit from LO to NLO, and by two units from NLO to $N^2\text{LO}$. The latter may stem from the partial inclusion of higher-order graphs in the partially re-summed integral equation. The ERE-parameterisation follows a weaker power-law than Z-parameterisation, indicating again greater cut-off sensitivity and less accuracy.

Thirdly, extrapolating the relative errors from the fit region, the cut-off variations at NLO and $N^2\text{LO}$ become comparable at $k \sim 150 - 200$ MeV, matching the estimate $\Lambda_{\neq} \sim m_\pi$.

order	n (Z-param.)	n (ERE-param.)
LO	1.8 – 2.1	
NLO	2.9	2.6
$N^2\text{LO}$	4.8	3.7
“ $N^2\text{LO}$ ”, $H_2 = 0$	3.1	2.8

Table 1: Fit of the logarithmic cut-off variation $\left|1 - \frac{k \cot \delta(\Lambda=200 \text{ MeV})}{k \cot \delta(\Lambda=1000 \text{ MeV})}\right|$ of $k \cot \delta$, shown in Fig. 4, for momenta higher than 70 and lower than 100 to 130 MeV to a power-law $(k/\Lambda_{\neq})^n$ for ERE- and Z-parameterisation at LO, NLO and $N^2\text{LO}$, and at $N^2\text{LO}$ without momentum-dependent three-body force H_2 . Varying the upper limit changes only the numbers for LO.

Finally, one confirms numerically the analytical finding in [12], recalled in Sect. 3.1, that a momentum-dependent three-body force H_2 enters at $N^2\text{LO}$ to increase accuracy. Setting $H_2 = 0$ does not only substantially increase the cut-off dependence of the $N^2\text{LO}$ -calculation, putting it close to the NLO dependence. As the slope at large momenta is also practically unchanged compared to the NLO value, H_2 is necessary to improve cut-off independence.

Notice that observables are at $N^2\text{LO}$ converged to be nearly cut-off independent, while the dimension-less three-body forces H_0 and H_2 vary dramatically even in a small window

⁵The deviation at $N^2\text{LO}$ to the potential-model results is at the same scale improved from 9.1% to 5.7%.

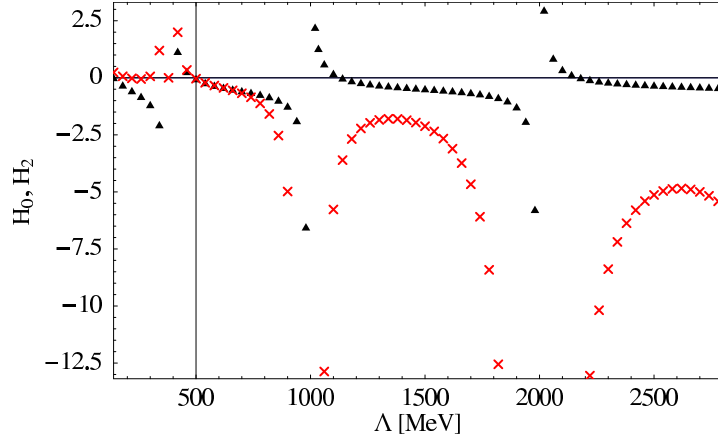


Figure 5: Dependence of the dimension-less three-body couplings at $N^2\text{LO}$ on the sharp momentum cut-off $\Lambda \in [140; 2800]$ MeV in Z-parameterisation. Triangles: $H_0(\Lambda)$; crosses: $H_2(\Lambda)$.

of cut-off variations, see Fig 5. The actual numerical values of H_0 and H_2 are quite sensitive to the regulator chosen, and to the precise values for $\gamma_{s/t}$ and $Z_{s/t}$ used. It is thus not the three-body forces which are large but the effect of variations in the cut-off Λ on observables. No simple connection between H_0 and H_2 exists at $N^2\text{LO}$, except that they both show a limit-cycle with the same period, which depends on $\gamma_{s/t}$ and $Z_{s/t}$.

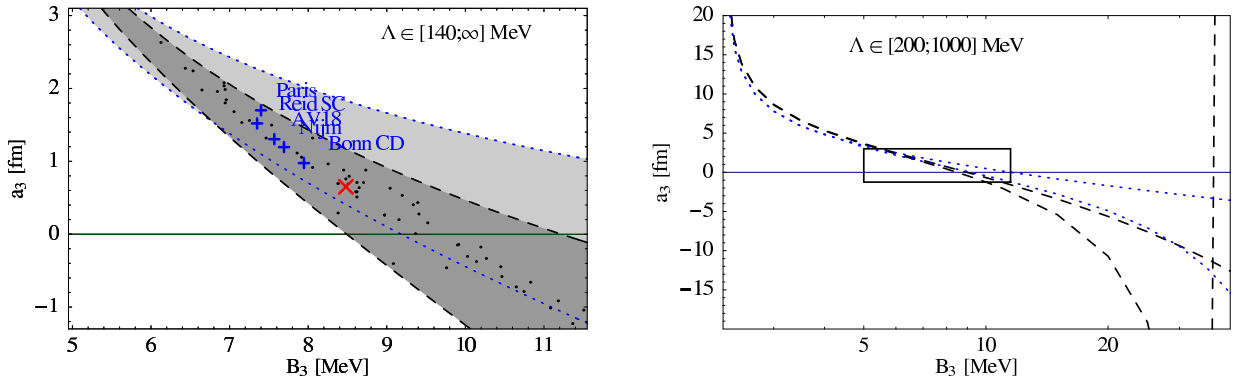


Figure 6: Prediction for the Phillips line at LO (dotted; lightly shaded region) and NLO (dashed; dark shaded region) in Z-parameterisation when the cut-off is varied in the region $\Lambda \in [140; 1000]$ MeV. Left: The dots correspond to the predictions for the triton binding energy and doublet scattering length in different models with the same two-body scattering lengths and effective ranges as inputs [40]. \times : experimental result. The outcome in various modern high-precision NN -potentials is indicated by crosses [41]. Right: Larger range, the rectangle showing the region covered on the left.

To complete the discussion, Fig. 6 displays the NLO-prediction for the Phillips line

in Z-parameterisation, compared to various old and modern potential model calculations which share the same two-body on-shell Physics. In the three-body system, their widely different off-shell behaviour predicts however different three-body bound state energies and Nd scattering lengths. The correlation between scattering length and bound state energy was first discussed by Phillips [42] and explained by Efimov [40]. The spread induced by varying the cut-off between 140 and 1000 MeV covers the off-shell dependence of all potential models. Note the pole in the scattering length at $B'_d \approx 36$ MeV at NLO for a cut-off $\Lambda = 1000$ MeV. This intrusion of another bound triton state is however outside the range of applicability of EFT($\not\!t$). As $k_{\text{typ}} \approx 180$ MeV $\gg \Lambda_{\not\!t}$ and the widths of the LO and NLO band are comparable, the EFT-calculation has not converged there.

3.4 Including the Effective Range to All Orders?

Why not re-sum all effective-range parameters up to a given order and replace the expanded version of the two-body scattering amplitudes (2.12) with the version (2.6/2.21),

$$D_{s/t}(p_0, \vec{p}) \xrightarrow{?} \frac{1}{\gamma_{s/t} - \frac{\rho_{0s/t}}{2}(\gamma_{s/t}^2 + \frac{\vec{p}^2}{4} - Mp_0) - \sum_{n=1}^{\infty} \rho_{ns/t}(\gamma_{s/t} + \frac{\vec{p}^2}{4} - Mp_0)^{n+1} - \sqrt{\frac{\vec{p}^2}{4} - Mp_0}} , \quad (3.23)$$

possibly with all coefficients after $\rho_{ns/t}$ set to zero at $N^{2n+1}\text{LO}$? This would immediately restore all effective-range corrections, give the correct pole residues, and is mandatory if $\rho_0\gamma \approx 1$. With this re-summation, the scattering length in the ${}^4S_{\frac{3}{2}}$ -channel and phase-shifts of the higher partial waves [15, 17, 19, 43, 44] were found with an accuracy of $\lesssim 4\%$. It was later also shown to simplify analytical calculations in the two-nucleon system [16].

However, the improvement in accuracy is only superficial: The higher ERE-parameters $\rho_{ns/t}$ are known with less and less accuracy, and other higher-order terms like P-wave interactions and relativistic corrections are still not included.

More severely, the propagator (3.23) has additional spurious poles, see Table 2: one for each S-wave at NLO ($\rho_{0s/t} \neq 0$), and two more at $N^3\text{LO}$ ($\rho_{1s/t} \neq 0$). Their positions change as more parameters $\rho_{ns/t}$ are included, and their residues add with the residue of the low-lying real and virtual bound state to zero. Albeit they all lie strictly speaking outside the range of validity of EFT($\not\!t$), $\gamma_{\text{spur},s/t} > \Lambda_{\not\!t}$, they are in particular in the 1S_0 -channel close enough to influence observables at momenta k above the break-up threshold, in particular as the closest of the spurious bound states have rather large residues. Recall that the half-off-shell amplitude goes to zero in the ${}^2S_{\frac{1}{2}}$ -channel only slowly, $\mathcal{A}(k, p) \propto 1/p$ [25, 27].

In the Nd -system, these additional poles generate new cuts in the solution to the integral equations: In the doublet channels, they conspire to pose an additional technical problem when one performs a rotation of the integration contour into the complex plane in the Hetherington-Schick procedure. On the other hand, expanding the two-particle propagator to a given order as in (2.19), only the physical pole with $\gamma_{s/t} \ll \Lambda_{\not\!t}$ is found in the two-particle scattering amplitude, and all problems with spurious bound-states are easily avoided.

Most severely, the asymptotic behaviour of the two-nucleon propagator is changed from $1/p$ to $1/p^2$ at large $p \gg 1/\rho_{0s/t}$. This leads to a non-trivial modification of the argument

order	3S_1 -channel		1S_0 -channel	
	$\gamma_{\text{spur},t}$ [MeV]	$Z_{\text{spur},t}$	$\gamma_{\text{spur},s}$ [MeV]	$Z_{\text{spur},s}$
NLO	178	−1.69	152	−0.90
N^3LO	−385 $170 \pm 108 i$	−0.14 $−0.77 \mp 0.60 i$	133 $−62 \pm 351 i$	−0.71 $−0.10 \mp 0.12 i$

Table 2: Binding momentum $\gamma_{\text{spur}} = \sqrt{MB_{\text{spur}}}$ and dimension-less residue analogous to (2.10/2.20) of the additional spurious bound states in the 3S_1 - and 1S_0 -scattering amplitudes when the effective-range parameters are re-summed as in (3.23).

for the inclusion of a three-body force in the $^2S_{\frac{1}{2}}$ -channel, as the resulting integral equation is then not analytically soluble in the UV-limit. Therefore, it is not straight-forward to construct analytically the cut-off dependence of the three-body force as in [12, 21] and demonstrate that it solves the Thomas problem of an attractive $1/r^2$ -potential. Gabbiani argued that with the kernel becoming less attractive, behaving only like $1/p^2$ (i.e. in position space like the Coulomb potential $1/r$), the cut-off sensitivity of the Wigner- $SU(4)$ symmetric component (3.13) of the integral equation in this channel disappears [45]. Thus, he claims that no limit cycle is found, and no three-body force is needed to achieve cut-off independence. According to him, the resulting phase-shifts without three-body forces in the $^2S_{\frac{1}{2}}$ -channel fail however miserably. I cannot confirm these findings but see that the phase-shifts in the $^2S_{\frac{1}{2}}$ -channel are markedly cut-off sensitive even at high Λ , and that three-body forces are necessary when the effective range is included to all orders. These findings will be discussed in a sub-sequent article [46].

Re-summing the effective-range corrections poses therefore numerically as well as technically non-trivial problems most importantly in the $^2S_{\frac{1}{2}}$ -wave (but also in the higher doublet-channels) while no increase in accuracy is achieved. To insert on the other hand the expanded two-nucleon amplitudes (2.19) in the kernel of the integral equation, as proposed in [12] and done here is a straightforward way to calculate phase-shifts to high accuracy, free of the problems mentioned above. In the end, all regularisation and re-summation schemes – including those which generate spurious bound states outside the range of validity of the EFT – must agree to the order of accuracy of the calculation. They must also have the same number of independently fixed three-body forces. To set up a consistent power-counting scheme and computations with good numerical convergence in a particular version can however be cumbersome and time-consuming.

3.5 More Partial Waves

After discussing the merits of Z-parameterisation in the only channel in which a three-body force enters already at LO and which exhibits a bound state of three nucleons, we now turn to the other partial waves. The solutions of the integral equations (3.1/3.4) for the real and

imaginary parts of the phase-shifts are displayed in Fig. 7 for the doublet channel, and in Fig. 9 for the quartet channel. The quartet-S wave is shown separately in Fig. 8. In the following, they are compared to potential-model calculations, and their convergence from order to order is discussed and juxtaposed with the phase-shifts obtained when the effective range is included to all orders. Table 3 lists low-energy parameters of lower partial waves.

Previous work on the higher phase-shifts in the Nd -system in EFT(\not{f}) focused mainly on the $^4S_{\frac{3}{2}}$ -channel, where pd -scattering [44] and the scattering length [15, 19, 43] and phase shifts [15, 17, 19] of nd -scattering were computed up to $N^2\text{LO}$. The phase-shifts of the other partial waves were presented in Ref. [17] to $N^2\text{LO}$. The NLO-results of [15] and [17] were obtained in “strict perturbation”, i.e. sandwiching the NLO-correction to the deuteron propagator proportional to $c_{0s/t}$ once between the LO-solution to the half-off-shell amplitude. Ref. [17] used already the Z-parameterisation to fix c_{0t} at NLO. In each case, the $N^2\text{LO}$ -calculations were carried out with the re-summed deuteron propagator (3.23).

Here, we use as in the $^2S_{\frac{1}{2}}$ -channel Z-parameterisation at each order and include perturbatively all corrections up to NLO and $N^2\text{LO}$ respectively into the kernel of the integral equation. As already discussed in Sect. 3.1, this contains some higher-order effects and leads to technical simplifications but – like a re-summed deuteron propagator – not to increased accuracy. The goal is again to show that convergence and agreement with data is improved.

Like in the discussion of the $^2S_{\frac{1}{2}}$ -wave in Sect. 3.3, the $N^2\text{LO}$ -results are compared to phase-shifts of a modern high-precision NN -potential. Numbers for nd -scattering using the AV18-potential with the Urbana IX-three-body-force were reported by Kievsky et al. [37, 38] and Hüber et al. [47, 48]. Within the drawing accuracy, they agree with the phase-shifts reported for the Nijmegen potentials 93, I and II, and for CD Bonn [48]. As the partial waves do not mix in EFT at $N^2\text{LO}$, the potential-model results for the $^{2s+1}l_j$ -partial waves were grouped into bins of fixed spin s and angular momentum l , with total angular momenta $j = l \pm \frac{1}{2}$ in the doublet channel, and $j = l \pm \{\frac{1}{2}; \frac{3}{2}\}$ in the quartet.

The higher the partial wave, the better the agreement with the potential model calculations. This comes as no surprise, since the strong centrifugal barrier for large angular momenta eliminates sensitivity on short-distance physics and the solution to the integral equation approaches the result of the Born approximation.

The EFT-calculation reproduces of course the well-known behaviour of the phase shifts at small momenta, e.g. [34],

$$k^{2l+1} \cot \delta^{(l)} \rightarrow -\frac{1}{\kappa_0^{(l)}} + \frac{\kappa_1^{(l)}}{2} k^2 + \mathcal{O}(k^4) \quad \forall k \rightarrow 0 \ , \quad (3.24)$$

where the S-wave parameters $\kappa_0^{(0)}$ and $\kappa_1^{(0)}$ are the scattering length a and effective range r_0 , the P-wave parameter $\kappa_0^{(1)}$ the scattering volume, etc. Table 3 lists parameters for low partial waves of the Nd -system. The theoretical accuracy may be estimated conservatively by $Q \sim \frac{\gamma_t}{m_\pi} \approx \frac{1}{3}$ of the difference between the NLO- and $N^2\text{LO}$ -result, or by the difference to the $N^2\text{LO}$ -result with re-summed effective-range corrections as in (3.23), since all $N^2\text{LO}$ -calculations must agree within the $N^2\text{LO}$ -accuracy. In the doublet channel, no re-summed

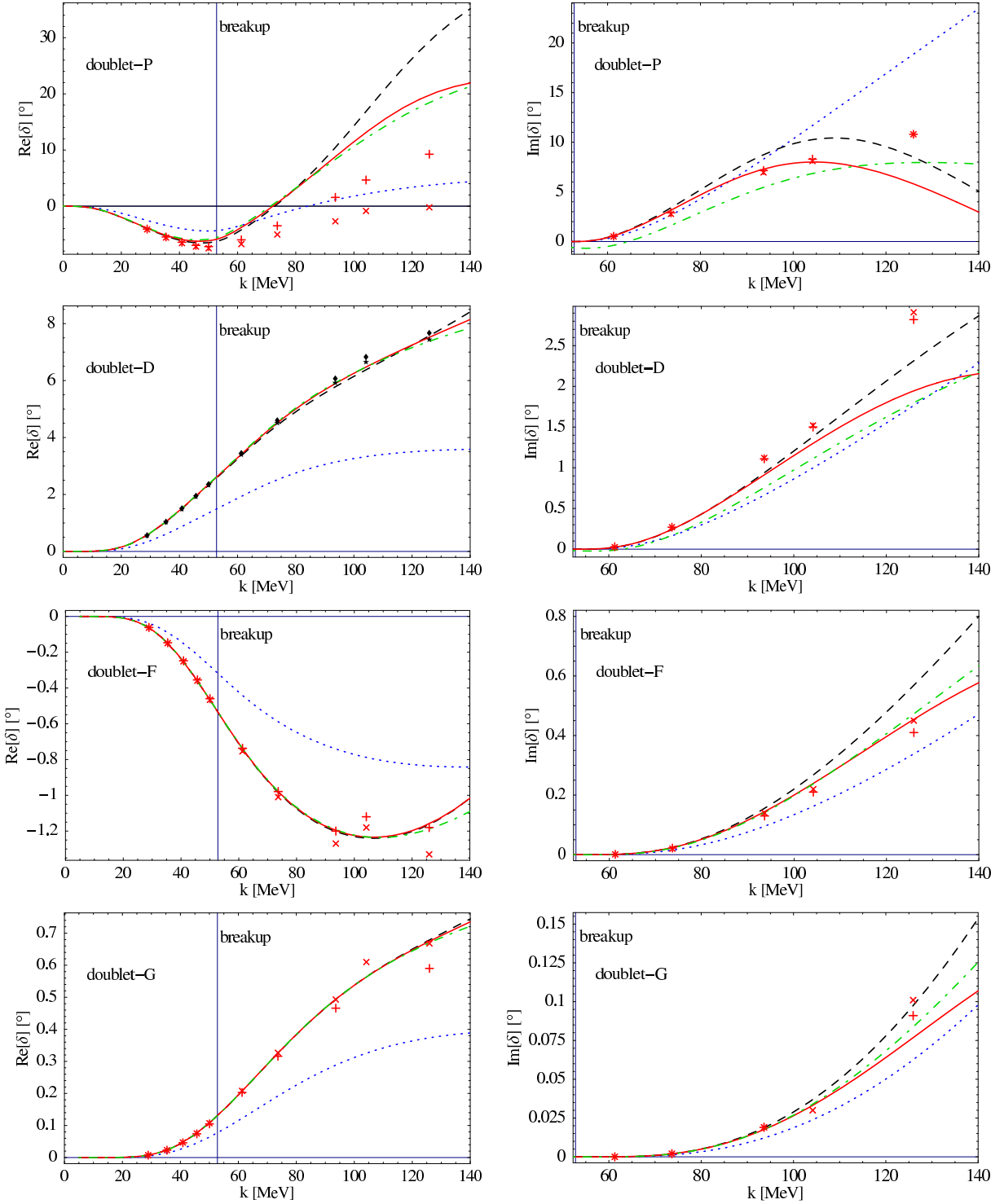


Figure 7: Real (left) and imaginary (right) part of the phase-shifts of the higher partial waves in the doublet channel in Z-parameterisation as function of the cm momentum k , $\Lambda = 1000$ MeV. Dotted: LO; dashed: NLO; solid: N^2 LO; dot-dashed: effective-range corrections summed to all orders. Result of AV18 + U IX from [37] below break-up, from [47] above, and at $k = 104$ MeV from [48]. 2l_j wave denoted by \times : $j = l - \frac{1}{2}$; $+$: $j = l + \frac{1}{2}$.

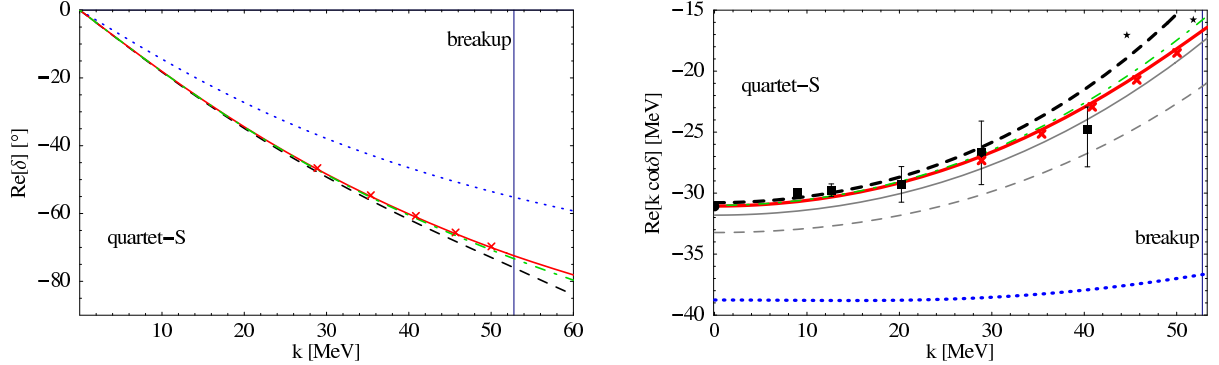


Figure 8: Phase-shift in Z-parameterisation (left) and comparison of ERE- and Z-parameterisation for $k \cot \delta$ (right) of the $^4S_{\frac{3}{2}}$ -wave as function of the cm momentum k ; $\Lambda = 1000$ MeV. Notation as in Figs. 7 and 4, and in addition on the right: boxes/stars: partial wave analysis [36] (for points with error-bars as reported in [42]); dot at $k = 0$: measured scattering length [31].

quartet-S		a [fm]		r_0 [fm]
order		Z-param.	ERE-param.	Z-param.
LO		5.091		-0.1
NLO		6.410	5.938	1.95
N^2 LO		6.354 ± 0.02	6.204	1.8 ± 0.1
experiment [31]		6.35 ± 0.02		
modern NN -potentials [41, 50]		6.34 ... 6.35		
N^2 LO re-summed, cf. [15, 19, 43]		6.365		1.8

	doublet-P		doublet-D	quartet-P		quartet-D
order	κ_0 [fm 3]	κ_1 [fm $^{-1}$]	κ_0 [fm 5]	κ_0 [fm 3]	κ_1 [fm $^{-1}$]	κ_0 [fm 5]
LO	33.1	-3.2	-268	-76.7	1.0	531
NLO	53.8	-2.1	-456	-139	0.45	894
N^2 LO	53.2 ± 0.2	-2.1	-456	-141	0.45	894
N^2 LO re-summed				-140	0.45	894

Table 3: The effective-range parameters (3.24) of the low partial waves in the Nd -system from Z-parameterisation in the first three orders. The result is un-changed under cut-off variations $\Lambda \in [200; 1000]$ MeV; theoretical accuracy discussed in the text.

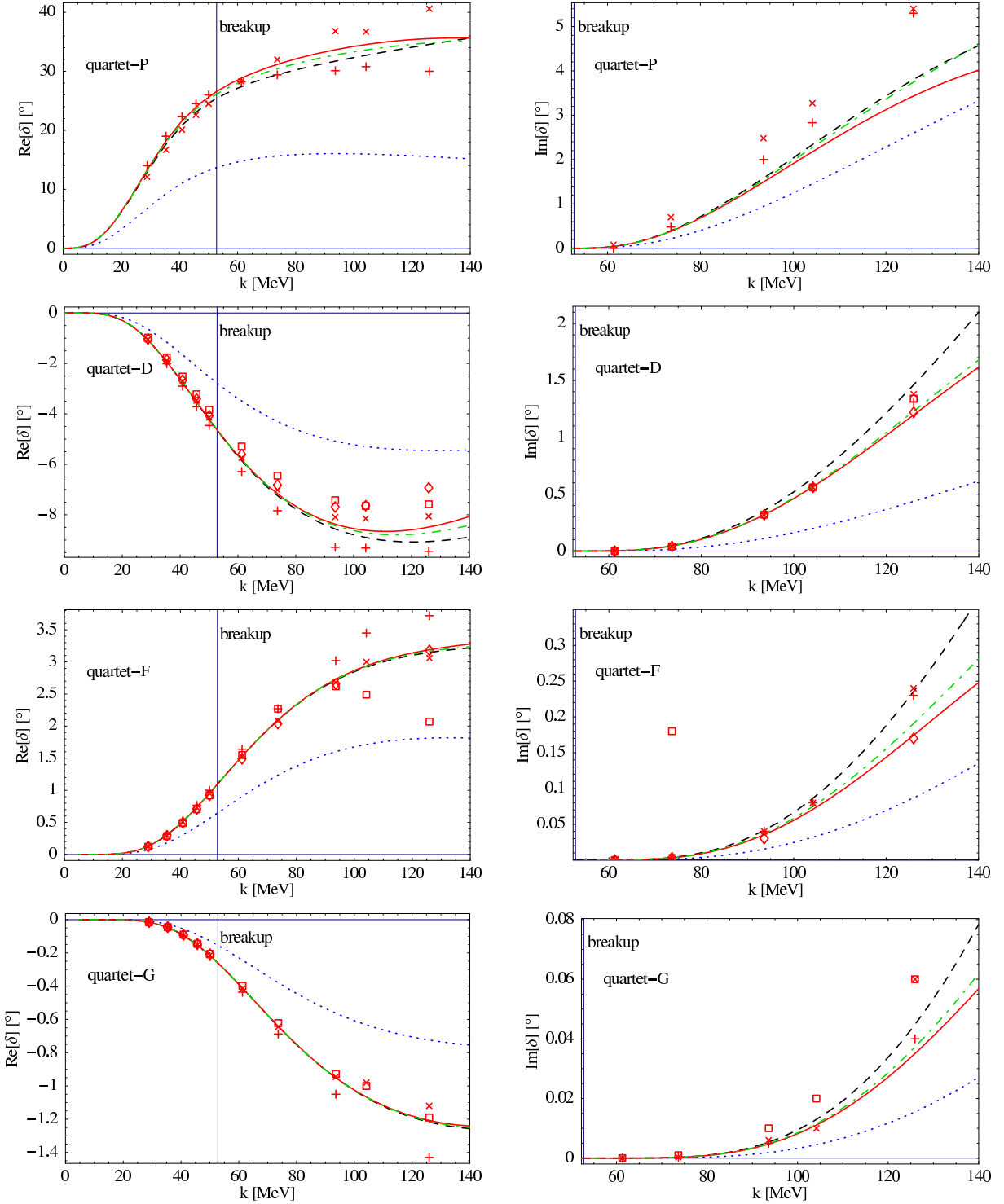


Figure 9: Real (left) and imaginary (right) part of the phase-shifts of the higher partial waves in the quartet channel in Z -parameterisation as function of the cm momentum k , $\Lambda = 1000$ MeV. Notation as in Fig. 7, and \square : $j = l - \frac{3}{2}$; \diamond : $j = l + \frac{3}{2}$ for the 4l_j -wave.

results are given due to the non-trivial cut-structure induced by the spurious poles of the two-nucleon propagators, see Sect. 3.4. Furthermore, no numbers are presented for the $^2S_{\frac{1}{2}}$ -channel as the measured scattering length (3.10) is used to determine the strength of the three-body force, and the effective range is very large, ~ 500 fm, rendering an effective-range expansion useless for this partial wave. In the other partial waves, the parameters involve the typical length scale $\sim 2 \dots 5$ fm, so that an effective-range expansion is often useful for momenta up to the deuteron break-up, $k_{\max} \lesssim 20 \dots 52$ MeV. More effective-range parameters are obtained without difficulty, but they are less likely to be measurable in the upcoming partial wave analysis of the nd -system [54].

The quartet-S wave scattering length has drawn substantial interest recently as its knowledge sets at present the experimental uncertainty in a recent, indirect determination of the doublet scattering length (3.10) [49]. At $N^2\text{LO}$, the result of Z-parameterisation in $\text{EFT}(\not{\pi})$ (using a perturbatively expanded kernel which is the inserted into the integral equation), $[6.35 \pm 0.02]$ fm, agrees very well with experiment [31] and modern high-precision potential-model calculations (which give $a_q = [6.34 \dots 6.35]$ fm) [41, 50], albeit partial-wave mixing, iso-spin breaking and electro-magnetic effects are not present in $\text{EFT}(\not{\pi})$ at $N^2\text{LO}$. a_q is obviously to a very high degree sensitive only to the correct asymptotic tail of the deuteron wave function, as comparison between the NLO result with its correct deuteron residue, the $N^2\text{LO}$ -result and the result of the re-summed deuteron propagator shows. As the amplitude decays at large off-shell momenta as $1/p^{3.17\dots}$ [19], this is not surprising.

Comparing $k \cot \delta$ in this partial wave at low energies in Fig. 8, the ERE-version converges much slower than the result of Z-parameterisation. For example, the $N^2\text{LO}$ -scattering length differs from experiment and the Z-parameterisation result of the same order still by 2%, and the correction from NLO to $N^2\text{LO}$ is with 5% much larger than the correction in Z-parameterisation. Indeed, partial $N^3\text{LO}$ - and $N^4\text{LO}$ -calculations in ERE-parameterisation which include only effective-range effects bring one slowly closer to the experimental number:

$$a^{(4S)}_{\text{ERE}} = (\underbrace{5.09}_{\text{LO}} + \underbrace{0.84}_{\text{NLO}} + \underbrace{0.27}_{\text{N}^2\text{LO}} + \underbrace{0.10}_{\text{"N}^3\text{LO}''} + \underbrace{0.04}_{\text{"N}^4\text{LO}''} + \dots) \text{ fm} \approx 6.34 \text{ fm} \quad (3.25)$$

The re-summed effective-range result of $\text{EFT}(\not{\pi})$ at $N^2\text{LO}$ was first reported in [15, 19, 43]. The ERE-result at NLO in [15], 6.7 fm, was found not by re-summing the expanded kernel as here, but by inserting the NLO-correction only once between the LO amplitudes. Thus, convergence is also sped up by iterating the perturbed kernel.

EFT shares also the rather complex structure found even at low k , e.g. in the doublet- and quartet-D and -F waves. Some disagreement with the potential-model results is seen in some imaginary parts at rather high momenta $k \gtrsim 120$ MeV, close to the breakdown scale of $\text{EFT}(\not{\pi})$, where the expansions parameter Q is approaching 1. Given that the imaginary parts are very small compared to the real parts and also most sensitive to details of the break-up reaction $nd \rightarrow nnp$, the overall agreement is not dis-encouraging. The most notable deviation occurs in the doublet-P wave, where internal convergence of the EFT-result is achieved up to more than $k \approx 100$ MeV, while significant deviations from data start around breakup. Clearly, more work is needed here.

While the NLO-corrections to the LO EFT-result are as expected rather large in Z-parameterisation, the N²LO-modifications are in the real parts of the phase-shifts tiny, and do not exceed 40% of the NLO corrections in the imaginary parts even as $k \rightarrow \Lambda_\pi \sim m_\pi$, the ²P-wave being again the only notable exception. The main difference between the strictly perturbative NLO-calculation of [17] which already utilised Z-parameterisation and the partially re-summed version used here is that now the NLO and N²LO-results lie practically on top of each other, while they noticeably differ in strictly perturbative Z-parameterisation above break-up. The difference does however never exceed 5%, and hence lies within the accuracy of the NLO calculation. The N²LO-results of [15, 17, 19] using the fully re-summed deuteron and ¹S₀-propagators (3.23) are nearly in-discernible from the partially re-summed version (2.19) in the real parts even at high k . In the imaginary parts, they do usually not deviate by more than 10% of the correction from NLO to N²LO at $k \sim 140$ MeV. This lies again well within the power-counting prediction that partial inclusion of N³LO-effects will not increase the accuracy of the N²LO-result. It gives however a band within which one expects a full N³LO-calculation to lie.

Finally, an unsolved technical issue has to be mentioned. The problem that the spurious poles of the re-summed two-body propagators induce additional cuts in the solution of the integral equation in the doublet channel, was already discussed in Sect. 3.4. Such breaches of unitarity below breakup, induced by naïve integration over a cut at high off-shell momenta, are the reason why the phase-shifts of the doublet-P and doublet-D-wave have a small non-zero value at the breakup point. As the half-off-shell amplitudes of higher partial waves converge substantially faster than of the doublet-S-wave, these violations become however less and less noticeable. For the higher partial waves, they disappear in the numerical noise.

To summarise, the overall convergence of the phase-shifts is good in all channels, both internally and to data. The only noticeable exception is the doublet-P-wave, in which the radius of convergence is limited to momenta k below break-up. Neglecting partial-wave splitting, simple observables like the differential cross-section do therefore agree with potential-model results and direct experimental measurements, within the level of accuracy of the EFT-prediction. As an illustration, the elastic differential cross-section is shown in Fig. 10 for three neutron energies: just below the *nd*-breakup ($k = 50$ MeV), and at two momenta close to the breakdown scale of EFT(π), $k \approx 90; 120$ MeV. The accuracy of the calculation is estimated by varying the N²LO-correction to $k \cot \delta$ by $Q \sim \gamma_t/m_\pi \approx 1/3$ around its central value. The agreement with experiments [51, 52] and potential-model calculations [37, 53] is quite satisfactory even close to the breakdown scale $k \sim m_\pi$. The main source of deviation is of course the insufficient description of the doublet-P-wave.

More complex variables need of course more refinement. For example, one obtains a zero-result for the nucleon-deuteron vector analysing power A_y in EFT(π) at N²LO because partial-wave splitting is absent. The well-known under-prediction of this observable in all modern, high-precision *NN*-potentials [2] – even when supplemented with three-body forces – is a challenge a higher-order EFT-calculation has to meet.

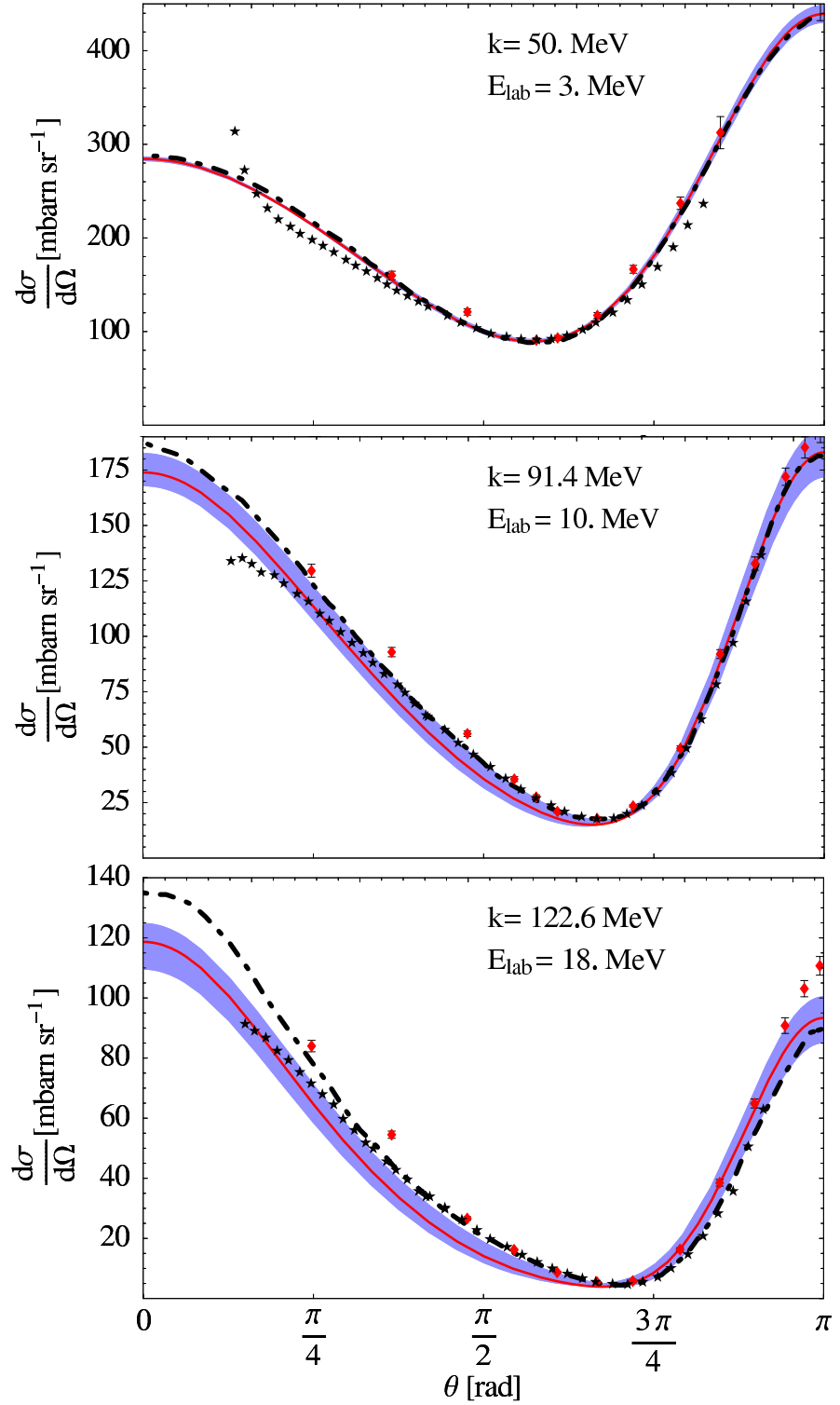


Figure 10: Elastic differential cross-sections of nd -scattering at N²LO in the cm-frame in Z-parameterisation (solid) with estimated accuracy (band). Dot-dashed: AV18 + Urbana IX from [37] at neutron kinetic energy $E_{\text{lab}} = 3 \text{ MeV}$, AV18 from [53] at $E_{\text{lab}} = 10; 18 \text{ MeV}$; diamonds: nd -data [51] (taken at 3; 10.25; 18 MeV); stars: pd -data [52].

4 Conclusions and Outlook

Z-parameterisation [13] fixes the parameters of “pion-less” Effective Field Theory at very low energies up to N²LO, i.e. up to an estimated theoretical accuracy of $\lesssim 3\%$, to the correct deuteron pole position and residue, instead of the effective-range parameters. As the asymptotic fall-off and normalisation of the deuteron wave-function at large distances is correctly reproduced, this improves drastically convergence in all processes in which the deuteron is either found as in- or out-state, or as sub-cluster of a more complex few-body system. The reason for the improvement is found in a rather large expansion parameter of $\gamma_t \rho_{0t} \approx 0.4$ for effective-range corrections, so that the deuteron residue is regained only up to 7% at N²LO when fitting to the effective range, while it is exact already at NLO in Z-parameterisation. Thus, the speed of convergence is faster, while the radius of convergence, set by the first scale on which new Physics enters, is of course not changed.

In this article, Z-parameterisation was extended and applied to deuteron-nucleon scattering, see Sects. 2 and 3.1. To perform the calculations, a computationally simple and convenient scheme was again employed which first expands the kernel to the desired order of accuracy in the power counting and then iterates it to all orders.

Numerical problems which origin from additional, spurious poles in the NN -amplitudes when the effective-range corrections are re-summed to all orders in the deuteron propagator are avoided in Z-parameterisation, Sect. 3.4. Therefore, standard techniques are readily applicable, and the calculation of scattering-observables also above break-up becomes computationally trivial, see a Mathematica-code at <http://www.physik.tu-muenchen.de/~hgrie>.

In all partial waves, the agreement of the phase-shifts with sophisticated potential-model calculations is increased in particular in the real and imaginary parts above the deuteron break-up point, see Sect. 3.5. What is more, the corrections from one order to the next in the EFT(\not{p})-expansion are smaller in Z-parameterisation, so that a partial re-summation of effective-range effects increases indeed the theoretical accuracy of the calculation. This allowed also for high-accuracy predictions of effective-range parameters in the low partial waves of the nd -system, which can be compared to an upcoming partial-wave analysis of the nd -system [54]. Most notably, the quartet-S wave scattering length is predicted as $a_q = [6.35 \pm 0.02]$ fm at N²LO, using only four observables from the NN -system as input, namely the asymptotic form and normalisation of the deuteron and virtual 1S_0 -bound state. This result compares both in magnitude and uncertainty favourably with the most advanced potential-model calculations ([6.34 … 6.35] fm [41, 50]), and with the experimental value ($[6.35 \pm 0.02]$ fm [31]). Simple observables like differential cross-sections are well reproduced as high as $E_{\text{lab}} \sim 15$ MeV.

The most striking success lies however in the $^2S_{\frac{1}{2}}$ -channel, which contains the triton as real bound state, Sect. 3.3. The numerical analysis of the cut-off dependence of its phase-shift in Z-parameterisation clearly supports the analytic finding in Ref. [12] that one and only one momentum-dependent three-body force enters at N²LO, namely the Wigner- $SU(4)$ -symmetric one with two derivatives. Fixing its strength to the triton binding energy, the accuracy of the calculation – deduced from the cut-off dependence of the answer – is improved at N²LO from $\sim 4\%$ to $\sim 1\%$ at a momentum scale of ~ 90 MeV typical for

the three-body system. The cut-off dependence follows in Z-parameterisation the pattern predicted by the power-counting. The difference to potential-model calculations is also substantially diminished.

The major source of uncertainty in the triton channel stems thus not from the theoretical accuracy of the EFT(π)-calculation, but from the error in the determination of its nd -scattering length, which is known only to $\sim 7\%$ accuracy. To reduce this uncomfortably large error bar to an accuracy of $\sim 0.7\%$ is the goal of an ongoing direct measurement of the incoherent scattering length at the Paul-Scherer-Institute [55]. A recent measurement of the bound coherent scattering length [49] relied for the extraction of $a_d = [0.645 \pm 0.003(\text{exp}) \pm 0.007(\text{theor})]$ fm on theoretical input for the $^4S_{\frac{3}{2}}$ -wave scattering length [50].

Future work includes a complete N^3LO -calculation, including iso-spin breaking effects and partial-wave splitting and mixing (which should improve in particular the doublet-P waves), the extension to include Coulomb interactions for the ^3He - and pd -system, and the coupling of electro-weak probes to the three-nucleon system. Not only will this allow for comparison with a cornucopia of data and help to shed light on long-standing puzzles like the A_y -problem. It will also lead to predictions with an accuracy relevant for nuclear astro-physics and neutrino physics at very low energies, contributing to the ongoing efforts to improve our knowledge about big-bang nucleo-synthesis, stellar evolution, neutrino-mass determinations and other fundamental processes of the Standard Model.

Acknowledgements

It is my pleasure to thank P. F. Bedaque, H.-W. Hammer, D. R. Phillips and G. Rupak for intense discussions and encouragement, and A. Kievsky and T. C. Black for communications about their results. N. Kaiser and W. Weise provided critical companionship. The warm hospitality and financial support for stays at the Nuclear Theory Group of Lawrence Berkeley National Laboratory, at the INT in Seattle and at the ECT* in Trento was instrumental for this research. In particular, I am grateful to the organisers and participants of the “Berkeley Visitors Programme on Effective Field Theories 2003” and of the “INT Programme 03-3: Theories of Nuclear Forces and Nuclear Systems”. This work was supported in part by the Bundesministerium für Forschung und Technologie, and by the Deutsche Forschungsgemeinschaft under contracts GR1887/2-1, 2-2 and 3-1.

A Deriving the Faddeev Equation

The Faddeev integral equation in the kinematics defined by Fig. 11 is

$$\begin{aligned} (t^{jB}{}_{iA})^{b\beta}_{a\alpha}(E; \vec{k}, \vec{p}) &= (K^{jB}{}_{iA})^{b\beta}_{a\alpha}(E; \vec{k}, \vec{p}) \\ &- \int \frac{d^3q}{(2\pi)^3} (K^{jB}{}_{lC})^{b\beta}_{c\gamma}(E; \vec{q}, \vec{p}) \mathcal{D}(E - \frac{\vec{q}^2}{2M}, \vec{q}) (t^{lC}{}_{iA})^{c\gamma}_{a\alpha}(E; \vec{q}, \vec{p}) , \end{aligned} \quad (\text{A.1})$$

where $E = \frac{3\vec{k}^2}{4M} - \frac{\gamma_t^2}{M}$ is the total non-relativistic energy in the cm-frame, \vec{k} (\vec{p}) the momentum of the incoming (outgoing) deuteron/spin-zero field with spin-isospin indices i/A (j/B), and the incoming (outgoing) nucleon has spin-isospin αa (βb). The integration over the loop-energy was already performed, setting $q_0 = \frac{\vec{q}^2}{2M}$ under the assumption that no additional poles above the real q_0 -axis are hidden in the interaction K . Sub-scripts (super-scripts) denote quantum numbers for incoming (outgoing) particles.

One decomposes now the integral equation into the pertinent spin-isospin and angular-momentum channels.

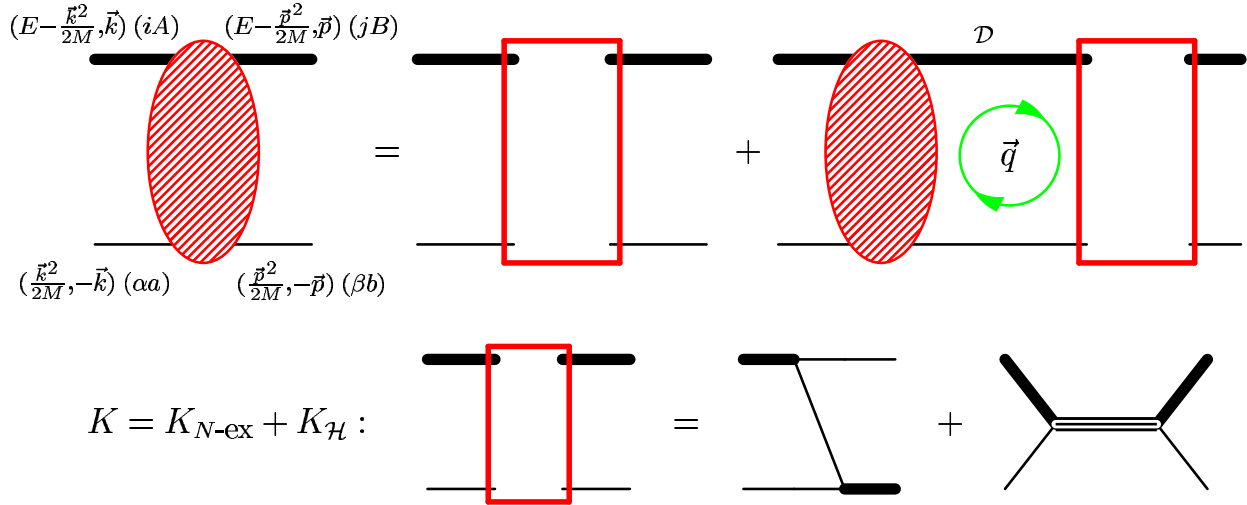


Figure 11: The Faddeev equation for Nd -scattering to N^2LO . Thick solid line: propagator of the two intermediate auxiliary fields d_s and d_t , denoted by \mathcal{D} , see (3.6); triple line: propagator of the triton auxiliary field t , see (3.17); K : interaction to N^2LO .

A.1 Projectors

As two cluster-configurations exist, namely Nd_t and Nd_s , it is convenient to decompose each operator (interactions, amplitudes etc.) as

$$\mathcal{O} = N_{b\beta}^\dagger \left(d_{t,j}^\dagger, d_{s,B}^\dagger \right) \begin{pmatrix} \mathcal{O}(Nd_t \rightarrow Nd_t)_i^j & \mathcal{O}(Nd_s \rightarrow Nd_t)_A^j \\ \mathcal{O}(Nd_t \rightarrow Nd_s)_i^B & \mathcal{O}(Nd_s \rightarrow Nd_s)_A^B \end{pmatrix}^{b\beta}_{a\alpha} \begin{pmatrix} d_t^i \\ d_s^A \end{pmatrix} N^{a\alpha} \quad (\text{A.2})$$

In other words, each operator is represented in cluster-configuration space by a 2x2-matrix which in addition carries spin- and iso-spin indices. It is understood in the following that the spin-isospin indices on the 2x2-matrix are applied to each entry separately, and that Kronecker- δ 's in spin or iso-spin are not displayed. Thus, for example, an entry $\mathcal{O}(Nd_t \rightarrow Nd_t) = \sigma_i \sigma^j$ in the above matrix is written out as

$$(\mathcal{O}(Nd_t \rightarrow Nd_t)^j{}_i)^{b\beta}{}_{a\alpha} = (\sigma_i \sigma^j)^{\beta}{}_{\alpha} \delta_a^b \quad (\text{A.3})$$

\mathcal{O} is usually not symmetric in any pair of spin-isospin indices (ij) , (AB) , $(\alpha\beta)$, (ab) .

The projection onto a state with angular momentum l , connecting momenta \vec{q}, \vec{p} with $\vec{q} \cdot \vec{p} = pq \cos \theta$ and $p = |\vec{p}|$ is as usual given by

$$\mathcal{O}^{(l)}(q, p) = \frac{1}{2} \int_{-1}^1 d\cos \theta \mathcal{O}(\vec{q}, \vec{p}) \ . \quad (\text{A.4})$$

Finally, the projectors onto the possible spin-isospin states of the three-nucleon system are: combining the auxiliary fields with spin-index i or iso-spin index A with a nucleon of spin-isospin α, a into the spin-doublet channel with spin μ and iso-spin m

$$(\mathcal{P}_{d,iA})^{m\mu}{}_{a\alpha} = \frac{1}{\sqrt{3}} \begin{pmatrix} \sigma_i & 0 \\ 0 & \tau_A \end{pmatrix}^{m\mu}{}_{a\alpha} , \quad (\text{A.5})$$

and into the spin-quartet channel with spin (μj) and iso-spin m

$$(\mathcal{P}_{q,i}^j)^{m\mu}{}_{a\alpha} = \begin{pmatrix} \delta_i^j - \frac{1}{3} \sigma^j \sigma_i & 0 \\ 0 & 0 \end{pmatrix}^{m\mu}{}_{a\alpha} . \quad (\text{A.6})$$

The projectors are related to their Hermitean conjugates by

$$\mathcal{P}_d^{iA} = (\mathcal{P}_{d,iA})^\dagger = \text{“}\mathcal{P}_{d,iA}\text{”} \ , \ (\mathcal{P}_{q,i}^j)^\dagger = \mathcal{P}_{q,j}^i \ , \quad (\text{A.7})$$

and are ortho-normalised:

$$\mathcal{P}_{d,iA} \mathcal{P}_d^{iA} = 1 \ , \ \mathcal{P}_{q,j}^k \mathcal{P}_{q,i}^j = \mathcal{P}_{q,i}^k \ , \ \mathcal{P}_{d,iA} \mathcal{P}_{q,j}^i = 0 \quad (\text{A.8})$$

For a complete set of spin-isospin projectors, supplement these by the (ortho-normalised) projector onto the iso-spin quartet channel with iso-spin (mB) and spin μ , which is not found in nucleon-deuteron scattering:

$$(\mathcal{P}_{\text{iso}q,A}^B)^{m\mu}{}_{a\alpha} = \begin{pmatrix} 0 & 0 \\ 0 & \delta_A^B - \frac{1}{3} \tau^B \tau_A \end{pmatrix}^{m\mu}{}_{a\alpha} , \ (\mathcal{P}_{\text{iso}q,A}^B)^\dagger = \mathcal{P}_{\text{iso}q,B}^A \quad (\text{A.9})$$

A.2 Projecting the Interaction Terms

The exchange of a nucleon is from the Lagrangeans (2.1/2.22/2.2) up to N²LO:

$$\left(K_{N\text{-ex}iA}^{jB}\right)_{a\alpha}^{b\beta}(E; \vec{q}, \vec{p}) = \frac{-My^2}{2} \frac{1}{p^2 + q^2 + \vec{p} \cdot \vec{q} - ME - i\epsilon} \begin{pmatrix} \sigma_i \sigma^j & \sigma^j \tau_A \\ \sigma_i \tau^B & \tau_A \tau^B \end{pmatrix}_{a\alpha}^{b\beta} \quad (\text{A.10})$$

The projection of the propagator of the exchanged nucleon onto angular momentum l is obtained by combining (A.4) with (3.2). There is no mixture between the doublet- and quartet-channels, and one finds in the doublet-channel

$$\mathcal{P}_{d,jB} \begin{pmatrix} \sigma_i \sigma^j & \sigma^j \tau_A \\ \sigma_i \tau^B & \tau_A \tau^B \end{pmatrix} \mathcal{P}_d^{iA} = \begin{pmatrix} -1 & 3 \\ 3 & -1 \end{pmatrix} \quad (\text{A.11})$$

and in the quartet

$$\mathcal{P}_{q,j}^l \begin{pmatrix} \sigma_i \sigma^j & \sigma^j \tau_A \\ \sigma_i \tau^B & \tau_A \tau^B \end{pmatrix} \mathcal{P}_{q,k}^i = 2 \mathcal{P}_{q,k}^l \quad (\text{A.12})$$

In cluster-configuration space, one obtains for the three-body interaction from (3.16)

$$\left(K_{\mathcal{H}}^{jB}{}_{iA}\right)_{a\alpha}^{b\beta}(E; \vec{q}, \vec{p}) = \frac{-My_3^2(\Lambda)}{3} \frac{1}{M\Omega - \sum_{n=1}^{\infty} \frac{h_{2n}(\Lambda)}{M^{n-1}} (ME + \gamma_t^2)^n} \begin{pmatrix} \sigma^j \sigma_i & -\sigma^j \tau_A \\ -\sigma_i \tau^B & \tau^B \tau_A \end{pmatrix}_{a\alpha}^{b\beta} \quad (\text{A.13})$$

By construction, the only non-zero contribution is in the doublet-S wave:

$$\mathcal{P}_{d,jB} \begin{pmatrix} \sigma^j \sigma_i & -\sigma^j \tau_A \\ -\sigma_i \tau^B & \tau^B \tau_A \end{pmatrix} \mathcal{P}_d^{iA} = 3 \begin{pmatrix} 1 & -1 \\ -1 & 1 \end{pmatrix} \quad (\text{A.14})$$

A.3 Result

Putting these results together and multiplying in the doublet-case the 2x2-matrix $t^{(l)}$ in cluster-configuration space from the right with the column vector $\begin{pmatrix} 1 \\ 0 \end{pmatrix}$, one projects finally onto the nucleon-deuteron system. There is no mixture or breaking between in- or out-states of different individual nucleon spin and iso-spin. One arrives thus finally at the integral equations for the quartet (3.1) and doublet (3.4) channels quoted in the main text.

References

- [1] G. E. Moore: *Electronics* **38**, No. 8 (April 19) (1965).
- [2] see e.g. D. Hüber and J. L. Friar, Phys. Rev. C **58**, 674 (1998) [nucl-th/9803038].
- [3] J. W. Chen, G. Rupak and M. J. Savage, Nucl. Phys. A **653**, 386 (1999) [nucl-th/9902056].
- [4] J. Schwinger, hectographed notes on nuclear physics, Harvard University 1947; G. F. Chew and M. L. Goldberger, Phys. Rev. **75**, 1637 (1949); F. C. Barker and R. E. Peierls, Phys. Rev. **75**, 3122 (1949); H. A. Bethe, Phys. Rev. **76**, 38 (1949).
- [5] V. Efimov, Nucl. Phys. A **362**, 45 (1981); Phys. Rev. C **44**, 2303 (1991); V. Efimov and E. G. Tkachenko, Phys. Lett. B **157**, 108 (1985).
- [6] S. Weinberg: Nucl. Phys. B **363**, 3 (1991).
- [7] see e.g. C. Ordoñez, L. Ray and U. van Kolck, Phys. Rev. C **53**, 2086 (1996) [hep-ph/9511380].
- [8] see e.g. E. Epelbaum, nucl-th/0309019; and references therein.
- [9] U. van Kolck, Prog. Part. Nucl. Phys. **43**, 337 (1999) [nucl-th/9902015].
- [10] S. R. Beane, P. F. Bedaque, W. C. Haxton, D. R. Phillips and M. J. Savage, in “At the frontier of particle physics”, M. Shifman (ed.), World Scientific, 2001 [nucl-th/0008064].
- [11] P. F. Bedaque and U. van Kolck, Ann. Rev. Nucl. Part. Sci. **52**, 339 (2002) [nucl-th/0203055].
- [12] P. F. Bedaque, G. Rupak, H. W. Grießhammer and H.-W. Hammer, Nucl. Phys. A **714**, 589 (2003) [nucl-th/0207034].
- [13] D. R. Phillips, G. Rupak and M. J. Savage, Phys. Lett. B **473**, 209 (2000) [nucl-th/9908054].
- [14] In EFT, this was first considered by D. B. Kaplan, Nucl. Phys. B **494**, 471 (1997) [nucl-th/9610052].
- [15] P. F. Bedaque and H. W. Grießhammer, Nucl. Phys. A **671**, 357 (2000) [nucl-th/9907077].
- [16] S. R. Beane and M. J. Savage, Nucl. Phys. A **694**, 511 (2001) [nucl-th/0011067].
- [17] F. Gabbiani, P. F. Bedaque and H. W. Grießhammer, Nucl. Phys. A **675**, 601 (2000) [nucl-th/9911034].

- [18] D. B. Kaplan, M. J. Savage and M. B. Wise, Nucl. Phys. B **534**, 329 (1998) [arXiv:nucl-th/9802075].
- [19] P. F. Bedaque, H.-W. Hammer and U. van Kolck, Phys. Rev. C **58**, R641 (1998) [nucl-th/9802057].
- [20] G. V. Skorniakov and K. A. Ter-Martirosian, Sov. Phys. JETP **4**, 648 (1957).
- [21] P. F. Bedaque, H.-W. Hammer and U. van Kolck, Nucl. Phys. A **676**, 357 (2000) [nucl-th/9906032].
- [22] I. S. Gradshteyn and I. M. Ryzhik, Table of Integrals, Series and Products, 5th edition; Academic Press, San Diego 1994.
- [23] H. W. Grießhammer, in: Mini-proceedings of “Chiral Dynamics: Theory and Experiment (CD2003),” eds. U.-G. Meißner, H.-W. Hammer and A. Wirzba, hep-ph/0311212; and in preparation.
- [24] L. W. Thomas, Phys. Rev. **47**, 903 (1935).
- [25] R. A. Minlos and L. D. Faddeev, Sov. Phys. JETP **14**, 1315 (1962).
- [26] G. S. Danilov, Sov. Phys. JETP **13**, 349 (1961).
- [27] P. F. Bedaque, H.-W. Hammer and U. van Kolck, Phys. Rev. Lett. **82**, 463 (1999) [nucl-th/9809025]; Nucl. Phys. A **646**, 444 (1999) [nucl-th/9811046].
- [28] K. G. Wilson, Phys. Rev. D **3**, 1818 (1971); S. D. Głazek and K. G. Wilson, Phys. Rev. D **47**, 4657 (1993); S. D. Głazek and K. G. Wilson, Phys. Rev. Lett. **89**, 230401 (2002) [hep-th/0203088].
- [29] E. Braaten and H. W. Hammer, Phys. Rev. Lett. **91**, 102002 (2003) [nucl-th/0303038].
- [30] E. Wigner, Phys. Rev. **51**, 106 (1937).
- [31] W. Dilg, L. Koester and W. Nistler, Phys. Lett. B **36**, 208 (1971).
- [32] H.-W. Hammer and T. Mehen, Phys. Lett. B **516**, 353 (2001) [nucl-th/0105072].
- [33] J. H. Hetherington and L. H. Schick, Phys. Rev. B **137**, 935 (1965); R. T. Cahill and I. H. Sloan, Nucl. Phys. A **165**, 161 (1971); R. Aaron and R. D. Amado, Phys. Rev. **150**, 857 (1966); E. W. Schmid and H. Ziegelmann, The Quantum Mechanical Three-Body Problem, Vieweg Tracts in Pure and Applied Physics Vol. 2, Pergamon Press (1974).
- [34] M. L. Goldberger and K. M. Watson, Collision Theory; John Wiley & Sons, New York 1964.
- [35] I. R. Afnan and D. R. Phillips, Phys. Rev. C **69**, 034010 (2004) [nucl-th/0312021].

- [36] W. T. H. van Oers and J. D. Seagrave, Phys. Lett. B **24**, 562 (1967).
- [37] A. Kievsky, S. Rosati, W. Tornow and M. Viviani, Nucl. Phys. A **607**, 402 (1996).
- [38] A. Kievsky, private communication.
- [39] G. P. Lepage, “How to renormalize the Schrödinger equation”, lectures given at 9th Jorge Andre Swieca Summer School: Particles and Fields, Sao Paulo, Brazil, 16-28 Feb 1997; nucl-th/9706029.
- [40] V. Efimov and E. G. Tkachenko, Few-Body Syst. **4**, 71 (1988).
- [41] H. Witała, A. Nogga, H. Kamada, W. Glöckle, J. Golak and R. Skibinski, nucl-th/0305028.
- [42] A. C. Phillips and G. Barton, Phys. Lett. B **28**, 378 (1969).
- [43] P. F. Bedaque and U. van Kolck, Phys. Lett. B **428**, 221 (1998) [nucl-th/9710073].
- [44] G. Rupak and X. W. Kong, Nucl. Phys. A **717**, 73 (2003) [nucl-th/0108059].
- [45] F. Gabbiani, nucl-th/0104088.
- [46] H. W. Grießhammer, in preparation.
- [47] D. Hüber, J. Golak, H. Witała, W. Glöckle and H. Kamada, Few-Body Syst. **19**, 175 (1995).
- [48] W. Glöckle, H. Witała, D. Hüber, H. Kamada and J. Golak, Phys. Rept. **274**, 107 (1996).
- [49] T. C. Black et al., Phys. Rev. Lett. **90**, 192502 (2003); K. Schön et al., Phys. Rev. C **67**, 044005 (2003).
- [50] J. L. Friar, D. Hüber, H. Witała and G. L. Payne, Acta Phys. Polon. B **31**, 749 (2000) [nucl-th/9908058].
- [51] P. Schwarz et al., Nucl. Phys. A **398**, 1 (1983).
- [52] K. Sagara et al., Phys. Rev. C **50**, 576 (1994).
- [53] A. Kievsky, M. Viviani and S. Rosati, Phys. Rev. C **64**, 024002 (2001) [nucl-th/0103058].
- [54] T. C. Black et al., in preparation.
- [55] B. van den Brandt, H. Glättli, H. W. Grießhammer, P. Hautle, J. Kohlbrecher, J. A. Konter and O. Zimmer, to be published in Nucl. Inst. Methds., nucl-ex/0401029.